

E-Values Expand the Scope of Conformal Prediction

Etienne Gauthier^{*1}, Francis Bach¹ and Michael I. Jordan^{1,2}

¹Inria, Ecole Normale Supérieure, PSL Research University

²Departments of EECS and Statistics, University of California, Berkeley

March 19, 2025

Abstract

Conformal prediction is a powerful framework for distribution-free uncertainty quantification. The standard approach to conformal prediction relies on comparing the ranks of prediction scores: under exchangeability, the rank of a future test point cannot be too extreme relative to a calibration set. This rank-based method can be reformulated in terms of p-values. In this paper, we explore an alternative approach based on e-values, known as conformal e-prediction. E-values offer key advantages that cannot be achieved with p-values, enabling new theoretical and practical capabilities. In particular, we present three applications that leverage the unique strengths of e-values: batch anytime-valid conformal prediction, fixed-size conformal sets with data-dependent coverage, and conformal prediction under ambiguous ground truth. Overall, these examples demonstrate that e-value-based constructions provide a flexible expansion of the toolbox of conformal prediction.

1 Introduction

Conformal prediction [Vovk et al., 2005] is a widely used statistical framework that provides predictive models with valid uncertainty quantification. The core objective is to construct conformal sets that, given features $X \in \mathcal{X}$, contain the true target $Y \in \mathcal{Y}$ with high probability.

These guarantees are distribution-free, meaning they hold under any underlying data-generating distribution \mathbb{P} , provided the data are exchangeable. Consider a dataset of n exchangeable data points $\{(X_i, Y_i)\}_{i=1, \dots, n}$, where each pair (X_i, Y_i) is drawn from some distribution $\mathbb{P} = \mathbb{P}_X \otimes \mathbb{P}_{Y|X}$ over $\mathcal{X} \times \mathcal{Y}$. This dataset, referred to as the calibration set, is used to construct conformal sets. Let $\alpha \in (0, 1)$ be a given error level. Given a new pair $(X_{n+1}, Y_{n+1}) \sim \mathbb{P}$ such that $(X_1, Y_1), \dots, (X_n, Y_n), (X_{n+1}, Y_{n+1})$ remain exchangeable, the objective is to construct a conformal set $\hat{C}_n(X_{n+1})$ satisfying

$$\mathbb{P}(Y_{n+1} \in \hat{C}_n(X_{n+1})) \geq 1 - \alpha, \quad (1)$$

where the probability is taken over both the calibration set $\{(X_i, Y_i)\}_{i=1, \dots, n}$ and the new data point (X_{n+1}, Y_{n+1}) .

In conformal prediction, uncertainty quantification relies on a score function $S : \mathcal{X} \times \mathcal{Y} \rightarrow \mathbb{R}$, which is typically derived from a pre-trained model f . The choice of S depends on the specific problem setting. In this work, we consider negatively-oriented scores, where smaller values indicate better performance, and assume these scores are positive.¹ An example of such a score is the cross-entropy loss used in classification tasks:

$$S(X, Y) = -\log p_f(Y|X), \quad (2)$$

where $p_f(Y|X)$ is the predicted probability assigned to the true class Y .

In standard conformal prediction methods, the idea is to rank nonconformity scores $S_i := S(X_i, Y_i)$ and compare their relative positions. This approach relies on the exchangeability of the scores, ensuring that

^{*}etienne.gauthier@inria.fr

¹The assumption that scores are negatively-oriented is not restrictive, as any positively-oriented score can be transformed, for example, via $S_{\text{negative}} = 1/(S_{\text{positive}} + \varepsilon)$ with ε preventing division by zero. Similarly, most scores used in conformal prediction are already nonnegative. We explicitly assume nonnegativity to simplify the construction of e-variables in conformal e-prediction, as in (4).

the rank of a new test point is unlikely to be overly extreme compared to those in the calibration set. For completeness, we include an overview of this classical framework in Appendix A.

Despite its theoretical appeal and simplicity, traditional conformal prediction faces significant limitations in practice. Some of these have to do with the lack of conditional guarantees, and there has been significant recent work aiming to address that limitation [Jung et al., 2023, Gibbs et al., 2024]. In the current paper, we highlight three additional scenarios where conventional methods fall short: batch anytime-valid conformal prediction, fixed-size conformal sets with data-dependent coverage, and conformal prediction under ambiguous ground truth. As we emphasize in the next three subsections, these scenarios all reflect real-world problems where one would like to make use of conformal methods. While conventional conformal prediction based on p-values falls short of addressing these problems, we will show that they are all solved by using e-values to construct conformal sets instead of p-values, a methodology known as *conformal e-prediction*. Our overall suggestion is that conformal e-prediction provides a flexible tool relative to classical conformal prediction that enhances the applicability of conformal methods in the complex, diverse, and dynamical settings of modern machine learning. The code implementation for our experiments is available at <https://github.com/GauthierE/evalues-expand-cp>.

1.1 Batch anytime-valid conformal prediction

In Section 2, we consider the following problem: data arrive sequentially in batches b_t , $t = 1, 2, \dots$, with each batch containing $n_t \geq 0$ calibration data points $S_1^t, \dots, S_{n_t}^t$ and a test data point $S_{n_t+1}^t$. Importantly, the batches arrive sequentially, one after the other, and the number of batches is possibly unknown in advance. Between batches, the data distribution may shift, meaning the data from one batch is not identically distributed with the next. We simply assume that the data within each batch, including both calibration and test data points, are exchangeable, conditional on the previous data batches.

Given $\alpha \in (0, 1)$, the goal is to construct a sequence of batch anytime-valid conformal sets \hat{C}_t for all $t \geq 1$, based on all past batches and the calibration data of batch t , satisfying:

$$\mathbb{P}(\forall t \geq 1, S_{n_t+1}^t \in \hat{C}_t) \geq 1 - \alpha, \quad (3)$$

where the probability is taken over all data points. If (3) holds, we call $\{\hat{C}_t\}_{t \geq 1}$ a sequence of batch anytime-valid conformal sets. As we now discuss, this problem arises in many real-life scenarios where data are received sequentially.

1.1.1 Motivating example 1: Pharmaceutical drug deployment across hospitals

A real-world example of this problem arises in pharmaceutical drug deployment across hospitals. A company introduces a new drug, and a regulatory agency seeks statistical guarantees on its efficacy. The drug’s effect on patient i in hospital b_t is denoted by S_i^t , where each hospital corresponds to a data batch. After an initial calibration phase in hospital b_t , where the drug is tested on n_t volunteer patients, the goal is to construct a conformal prediction set for $S_{n_t+1}^t$, representing a future patient in that hospital.

The deployment is inherently sequential: hospitals test the drug at different times, and results arrive progressively. The agency must provide anytime-valid statistical guarantees for all hospitals, constructing conformal prediction sets for future patients $S_{n_t+1}^t$ across all sites, regardless of how many batches t have been received.

Moreover, data distributions vary across hospitals due to differences in patient demographics, lifestyles, and medical histories. For instance, urban and rural hospitals may observe different drug efficacy patterns. The regulatory agency must account for these distributional shifts while leveraging prior batches to enhance predictive reliability.

1.1.2 Motivating example 2: Quality control in supply chains

In a production supply chain, a company regularly receives shipments of parts from a supplier. Each batch contains q_t units, each with a quality rating S_i^t , assessed by the company. The batch size q_t varies based on demand.

While unit quality within a batch is typically exchangeable, it may fluctuate across batches due to changes in the supplier’s production process (e.g., machinery wear) or transportation conditions. To manage this uncertainty, the company can apply batch anytime-valid conformal prediction to obtain quality

guarantees. Specifically, for each batch, it selects $n_t < q_t$ units to measure quality, forming a calibration set $S_1^t, \dots, S_{n_t}^t$. Then, it predicts the quality of a randomly chosen product $S_{n_t+1}^t$ from the remaining units. Since quality assessment is costly, n_t is typically small relative to q_t .

The key advantage of this method is its validity for any batch and any stopping time τ . The company can flexibly decide when to stop quality assessments, depending on prior observations. This adaptive approach helps optimize testing costs while ensuring reliable predictions, improving supply chain efficiency.

1.1.3 Limitations of traditional conformal prediction methods

The standard method in conformal prediction produces a conformal set \hat{C}_t for a batch of exchangeable data $S_1^t, \dots, S_{n_t}^t, S_{n_t+1}^t$ such that

$$1 - \alpha \leq \mathbb{P}(S_{n_t+1}^t \in \hat{C}_t) < 1 - \alpha + \frac{1}{n_t + 1},$$

where the rightmost inequality holds if the data are almost surely distinct. In dynamic scenarios such as batch anytime-valid conformal prediction, simply applying existing conformal prediction methods to each batch does not yield batch anytime-valid guarantees. We formalize this fact in the following lemma:

Lemma 1.1. *Let \hat{C}_t be the conformal set obtained using standard conformal prediction on batch b_t for any $t \geq 1$. Suppose that: (i) almost surely, there are no ties within any batch; (ii) batches are independent; and (iii) $n_t \geq \frac{2}{\alpha} - 1$ for all $t \geq 1$.*

Then, $\{\hat{C}_t\}$ is not a sequence of batch anytime-valid conformal sets.

Proof. Let $T := \left\lceil \frac{\log(1-\alpha)}{\log(1-\alpha/2)} \right\rceil$. We have:

$$\begin{aligned} \mathbb{P}(\forall t \geq 1, S_{n_t+1}^t \in \hat{C}_t) &\leq \mathbb{P}(\forall t = 1, \dots, T, S_{n_t+1}^t \in \hat{C}_t) \\ &= \prod_{t=1}^T \mathbb{P}(S_{n_t+1}^t \in \hat{C}_t) \\ &< \prod_{t=1}^T \left(1 - \alpha + \frac{1}{n_t + 1} \right) \\ &< (1 - \alpha/2)^T \leq 1 - \alpha. \end{aligned}$$

The equality comes from the fact that all sets \hat{C}_t depend only on data from batch b_t and batches are independent. The last two inequalities come from the assumptions on n_t and the definition of T respectively. \square

Standard conformal prediction methods do not provide simultaneous coverage guarantees for each batch when the number of batches is unknown in advance. Using a stricter coverage $\bar{\alpha} < \alpha$ combined with union bound does not solve this issue, as it requires knowing the number of batches beforehand. We will show how e-values address this issue in Section 2.

1.2 Fixed-size conformal sets with data-dependent coverage

Traditional conformal prediction methods operate by fixing a coverage level α in advance, ensuring that the true label falls within the conformal set with probability at least $1 - \alpha$. While this approach offers strong theoretical guarantees, it does not provide control over the size of the conformal sets, which can vary widely depending on the underlying data distribution.

Instead of fixing α a priori, we allow the coverage level $\tilde{\alpha}$ to adapt based on the data, tailored to yield conformal sets of desired size. We describe this adaptive approach in Section 3. It enables more flexible conformal sets that are better aligned with the specific instance being predicted, potentially improving the interpretability and usability of conformal prediction in real-world applications.

1.2.1 Motivating example: Medical diagnosis

In healthcare, doctors often rely on machine learning models to help identify potential diseases based on patient symptoms, medical history, and test results. Conformal prediction methods enhance these models by providing sets of possible diagnoses with confidence guarantees, assisting doctors in prioritizing further tests or treatments. However, due to time constraints and resource limitations, doctors can typically consider only a fixed number of diagnoses (e.g., the top three or four).

While statistically sound, the traditional conformal prediction approach does not control set size, which can vary significantly. In some cases, the set may be impractically large, while in others, it may be too small, risking missed diagnoses.

1.3 Conformal prediction under ambiguous ground truth

We will also discuss a third application of conformal e-prediction, which naturally addresses a problem introduced by [Stutz et al. \[2023\]](#).

In machine learning, labels are not always precisely known, particularly in scenarios where expert annotations are used. Instead of standard feature-label pairs (X_i, Y_i) , we may encounter (X_i, Y_i^j) for $j = 1, \dots, m$ where m is the number of experts providing predictions. This framework arises, for instance, in medicine, where a patient X_i is assessed by multiple experts, each predicting a diagnosis Y_i^j . Consequently, the samples become non-exchangeable, making traditional conformal prediction methods relying on rank-based statistics inapplicable.

This setting has been discussed by [Stutz et al. \[2023\]](#) under a framework they refer to as *Monte Carlo conformal prediction*. In their approach, the calibration set consists of features $X_i \sim \mathbb{P}_X$, and for each X_i , m labels $Y_i^j \sim \mathbb{P}_{Y|X_i}$, for $j = 1, \dots, m$. Consequently, the calibration set $\{(X_i, Y_i^j)\}_{i=1, \dots, n}^{j=1, \dots, m}$ no longer consists of exchangeable data, making the standard conformal prediction technique inapplicable.

To address this, [Stutz et al. \[2023\]](#) build on classical statistical results on p-variable averaging to provide a coverage guarantee of $1 - 2\alpha$. In Section 4, we suggest an alternative based on e-values for which we can establish theoretical guarantees for achieving a coverage of $1 - \alpha$. Thus an e-value-based approach can provide uncertainty quantification in this non-exchangeable setting.

1.4 A brief overview of conformal e-prediction

As we will show, compared to p-variables, on which most existing conformal prediction methods are based, e-variables offer greater flexibility and enable the construction of conformal sets in more complex settings.² We begin with a brief introduction to e-values and their usage in conformal prediction.

Definition 1.2 (e-variable). An *e-variable* E is a nonnegative random variable that satisfies

$$\mathbb{E}[E] \leq 1.$$

Coupled with probabilistic inequalities, well-designed e-variables based on the calibration set and the test data point enable the construction of relevant conformal sets. For instance, using Markov’s inequality, we obtain:

$$\mathbb{P}(E < 1/\alpha) = 1 - \mathbb{P}(E \geq 1/\alpha) \geq 1 - \alpha \mathbb{E}[E] \geq 1 - \alpha,$$

which allows for the construction of conformal sets satisfying (1).

Remark 1.3 (Terminology). For clarity, we will use the term *conformal p-prediction* for p-variable-based conformal prediction methods, rather than simply *conformal prediction* as is common in the literature. *Conformal e-prediction* refers to conformal prediction methods based on e-variables. The term *conformal prediction* broadly denotes the construction of conformal sets for a test point using a calibration set, regardless of the method.

Initially, in the 1990s, conformal prediction methods were introduced using e-variables (under different names, as the term e-variable only recently emerged in the literature). Over the years, conformal prediction methods based on p-variables gradually gained popularity. For a discussion on the advantages of e-variables and p-variables in conformal prediction, we recommend reading [Vovk \[2024\]](#), who provides

²We refer to “p-variables” and “e-variables” when discussing the underlying random variable, and “p-values” and “e-values” for the observed values.

a historical context on why p-variables came to dominate over e-variables in conformal prediction. While conformal p-prediction has been widely used, e-variables bring several fundamental advantages that can be advantageous. In this work, we leverage e-variables to produce valid conformal sets for the three case studies introduced earlier: batch anytime-valid conformal prediction, fixed-size conformal sets with data-dependent coverage, and conformal prediction under ambiguous ground truth. Although any e-variable can be used, for concreteness we adopt the following e-variable:

$$E = \frac{S_{n+1}}{\frac{1}{n+1} \sum_{i=1}^{n+1} S_i}, \quad (4)$$

which was introduced by [Balinsky and Balinsky \[2024\]](#), and which can be readily seen to have expectation equal to one under exchangeability.³ Using this e-variable in conformal prediction we directly compare the test data point's score with the average of all the scores, rather than comparing their ranks.

2 Batch Anytime-valid Conformal Prediction

The methods derived from e-statistics are powerful tools for statistical inference due to their connection with fundamental probabilistic inequalities. As discussed previously, a key starting point is Markov's inequality, which provides an upper bound on the tail probabilities of nonnegative random variables. A stronger result generalizing Markov's inequality is an inequality due to [Ville \[1939\]](#), which applies to nonnegative supermartingales and is central in sequential analysis and anytime-valid inference. To state Ville's inequality rigorously, we first define the concepts of filtrations and (super)martingales; see [Williams \[1991\]](#) for a standard reference.

Formally, we fix a probability space $(\Omega, \mathcal{F}, \mathbb{P})$, where Ω is a sample space, \mathcal{F} is a σ -algebra, and \mathbb{P} is a probability measure. We focus on real-valued random variables, defined as measurable functions mapping Ω to \mathbb{R} .

Definition 2.1 (Filtration). A *filtration* is a sequence $\{\mathcal{F}_t\}_{t \geq 0}$ of sub- σ -algebras of \mathcal{F} such that $\mathcal{F}_s \subseteq \mathcal{F}_t$ for all $s \leq t$.

Definition 2.2 (Martingale). Let $\{M_t\}_{t \geq 0}$ be a sequence of random variables. The sequence $\{M_t\}_{t \geq 0}$ is a *martingale* for the filtration $\{\mathcal{F}_t\}_{t \geq 0}$ if:

- M_t is \mathcal{F}_t -measurable for all $t \geq 0$,
- $\mathbb{E}[|M_t|] < +\infty$ for all $t \geq 0$,
- $\mathbb{E}[M_{t+1} | \mathcal{F}_t] = M_t$ (almost surely) for all $t \geq 0$.

If the equality $\mathbb{E}[M_{t+1} | \mathcal{F}_t] = M_t$ is replaced with the inequality $\mathbb{E}[M_{t+1} | \mathcal{F}_t] \leq M_t$, $\{M_t\}_{t \geq 0}$ is said to be a *supermartingale*. In particular, all martingales are supermartingales.

If the filtration is clear from context, we may say that $\{M_t\}_{t \geq 0}$ is a (super)martingale without explicitly specifying the filtration $\{\mathcal{F}_t\}_{t \geq 0}$. In this work, we focus on supermartingales with an initial value of $M_0 = 1$; these are usually referred to as *test supermartingales* (see, for example, [Waudby-Smith and Ramdas \[2023\]](#)). In this specific case, Ville's inequality can be stated as follows:

Theorem 2.3 (Ville's Inequality). *Let $\{M_t\}_{t \geq 0}$ be a nonnegative test supermartingale. Then, for any $\alpha \in (0, 1)$:*

$$\mathbb{P}(\forall t \geq 0, M_t < 1/\alpha) \geq 1 - \alpha.$$

A straightforward proof follows from the upcrossing lemma and the supermartingale convergence theorem of [Doob \[1953\]](#).

Remark 2.4 (Ville's Inequality with Stopping Times). A useful alternative formulation of Ville's inequality involves stopping times. Recall that a random variable τ taking values in $\mathbb{N} \cup \{\infty\}$ is a *stopping time* with respect to a filtration $\{\mathcal{F}_t\}_{t \geq 0}$ if $\{\tau \leq t\} \in \mathcal{F}_t$ for all $t \geq 0$, meaning that the decision to stop at time τ depends only on the information available up to t . Given a nonnegative test supermartingale $\{M_t\}_{t \geq 0}$, Ville's inequality extends to stopping times as follows:

$$\mathbb{P}(M_\tau < 1/\alpha) \geq 1 - \alpha,$$

³For a formal proof, see [Balinsky and Balinsky \[2024\]](#).

for any stopping time τ . This result ensures that the coverage guarantee holds regardless of when we stop the process based on the observed data. A proof of this equivalent reformulation can be found in Lemma 3 of [Howard et al. \[2021\]](#).

Ville's inequality provides a strong guarantee for nonnegative test supermartingales, bounding the probability that the process exceeds a threshold $1/\alpha$ at any time step. This makes it a crucial tool for constructing batch anytime-valid conformal sets.

2.1 Theoretical framework

To apply Ville's inequality, we first need a carefully chosen nonnegative test supermartingale, which in turn requires defining an appropriate filtration. Throughout this section, we will consider the filtration of sigma-algebras generated by all random variables from the data batches obtained so far. More precisely:

$$\begin{aligned}\mathcal{F}_1 &= \sigma(S_1^1, \dots, S_{n_1}^1, S_{n_1+1}^1), \\ \mathcal{F}_2 &= \sigma(S_1^1, \dots, S_{n_1}^1, S_{n_1+1}^1, S_1^2, \dots, S_{n_2}^2, S_{n_2+1}^2),\end{aligned}$$

and more generally:

$$\mathcal{F}_t = \sigma(S_1^1, \dots, S_{n_1}^1, S_{n_1+1}^1, \dots, S_1^t, \dots, S_{n_t}^t, S_{n_t+1}^t).$$

In particular, \mathcal{F}_0 is the trivial sigma-algebra $\{\emptyset, \Omega\}$. We can now define a sequence of random variables $\{M_t\}_{t \geq 0}$, which will be fundamental for defining our batch anytime-valid conformal sets. The definition of M_t is inspired by the e-variable in Equation (4) introduced by [Balinsky and Balinsky \[2024\]](#).

Theorem 2.5. *For all $t \geq 0$, the sequence of random variables $\{M_t\}_{t \geq 0}$ defined by:*

$$M_t = \prod_{s=1}^t E_s$$

where

$$E_s = \frac{S_{n_s+1}^s}{\frac{1}{n_s+1} \sum_{j=1}^{n_s+1} S_j^s}$$

for all $s \geq 1$, is a nonnegative test supermartingale.

Proof. First, by the definition of an empty product, we have that $M_0 = 1$. Now, since we have assumed in this work that the scores are positive, it is clear that $M_t \geq 0$ for all $t \geq 0$. The only thing left to prove is that $\{M_t\}_{t \geq 0}$ is a supermartingale. Let $t \geq 1$. We have:

$$\mathbb{E}[M_t | \mathcal{F}_{t-1}] = \mathbb{E} \left[\prod_{s=1}^t E_s \middle| \mathcal{F}_{t-1} \right] = \underbrace{\left(\prod_{s=1}^{t-1} E_s \right)}_{=M_{t-1}} \mathbb{E}[E_t | \mathcal{F}_{t-1}]$$

and see that $\mathbb{E}[E_t | \mathcal{F}_{t-1}] = 1$ since we assumed that, within a given batch, the data are exchangeable, conditional on the previous data batches. A proof of this fact can be found in [Balinsky and Balinsky \[2024\]](#). Therefore, $\{M_t\}_{t \geq 0}$ is a martingale, and thus, in particular, a supermartingale. \square

Therefore, by applying Ville's inequality to the test supermartingale $\{M_t\}_{t \geq 0}$, we deduce the following corollary.

Corollary 2.6. *For $t \geq 1$, let \hat{C}_t be the subset of \mathbb{R} defined by:*

$$\hat{C}_t := \left\{ v \in \mathbb{R}_+ : \prod_{s=1}^{t-1} E_s \times \frac{v}{\frac{1}{n_t+1} \left(\sum_{j=1}^{n_t} S_j^t + v \right)} < 1/\alpha \right\}. \quad (5)$$

Thus $\{\hat{C}_t\}_{t \geq 0}$ is a sequence of batch anytime-valid conformal sets.

In the definition of \hat{C}_t , v serves as a placeholder for the random variable $S_{n_t+1}^t$. The set \hat{C}_t is constructed to ensure that $S_{n_t+1}^t$ falls within it with high probability.

Remark 2.7. We constructed the martingale M_t in Theorem 2.5 by simply taking the product of the e-variables E_s . While the product martingale has certain desirable properties, alternative constructions are possible. In particular, Theorem 2.5 extends naturally, and one can see that the cumulative product $M_t = \prod_{s=1}^t (1 - \lambda_s + \lambda_s E_s)$, where $\lambda_t \in [0, 1]$ is any measurable function of E_1, \dots, E_{t-1} , is also a martingale. This construction enjoys appealing theoretical properties, especially when using $\lambda_t = \arg \max_{\lambda \in [0, \gamma]} \frac{1}{t-1} \sum_{s=1}^{t-1} \log(1 - \lambda + \lambda E_s)$ for some $\gamma \in (0, 1]$. In this paper, we focus on the “all-in” process with $\lambda_t = 1$ for simplicity, but exploring these alternative processes would be worthwhile. For further details, we refer to Waudby-Smith and Ramdas [2023], Wang et al. [2024], Ramdas and Wang [2024]. This construction is closely related to the universal portfolio algorithm proposed by Cover [1991]; see also Vovk [1990], Cover and Ordentlich [1996], Vovk and Watkins [1998], Orabona and Jun [2023], Ryu and Bhatt [2024].

2.2 Experiments

In real-world machine learning applications, models are often deployed in dynamic environments where data arrives in a sequential or distributed manner. Unlike traditional static datasets where calibration is performed globally, real-world deployments often require incremental calibration as new users interact with the system.

For our experiments, we use the Federated Extended MNIST (FEMNIST) dataset, a standard benchmark in federated learning and image classification [Caldas et al., 2018]. FEMNIST extends the EMNIST dataset [Cohen et al., 2017], itself derived from MNIST [LeCun, 1998], and includes 62 classes: digits (0-9) and uppercase and lowercase letters (A-Z, a-z). Originally designed for federated learning, where data are distributed non-i.i.d. across clients, we adapt it by treating each writer as a data batch. The dataset consists of 3,597 clients—each representing a unique writer—with varying numbers of samples, introducing natural heterogeneity and imbalance. We leverage this structure to simulate scenarios where data arrives in groups with inherent variability. The dataset is split into a training set of approximately 650,000 images and a test set of about 165,000 images, with distinct writers in each set to prevent overlap. Each image is a 28×28 grayscale representation, consistent with the original MNIST format.

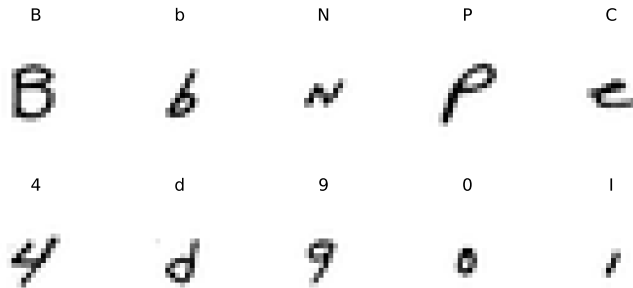


Figure 1: Some images from FEMNIST with their associated class label.

We train a convolutional neural network f , inspired by LeNet [LeCun et al., 1998] and adapted for our 62-class recognition task. This simple model serves as a black-box predictor to evaluate the effectiveness of our conformal prediction method⁴. Details on the architecture and training parameters are provided in Appendix B. On the test set, f achieves 87.6% accuracy.

The test set consists of multiple writers, each contributing a variable number of image samples. To implement our batch anytime-valid conformal prediction method, we proceed as follows. We randomly select $T = 50$ writers from the test set to serve as data batches. Since the dataset is finite, we run our method for a fixed number of batches, 50 in this case, but the approach extends to any T . We then split the test set into two equal parts: a calibration set (50% of the original test data) and a final test set (the remaining 50%).

Conformal sets are constructed sequentially. At step $t = 1$, for the first selected writer, we extract the calibration scores $S_1^1, \dots, S_{n_1}^1$, where n_1 is the number of samples from that writer in the calibration set.

⁴Since conformal prediction is model-agnostic, its validity holds regardless of the underlying model. Therefore, we use a standard, well-understood model rather than a state-of-the-art architecture. This choice ensures that the observed coverage behavior stems from the conformal method itself rather than from improvements in the base model’s accuracy.

Using these scores, we construct a conformal prediction set following (5). Next, we sample a test point $S_{n_{t+1}}^1$ from the final test set corresponding to the same writer and evaluate the e-variable E_1 . We repeat this process for each subsequent writer ($t = 2, 3, \dots, 50$).

The choice of the score function S is key to obtaining informative conformal sets. In particular, S should be chosen so that the martingale M_t in Theorem 2.5 does not decay to zero too quickly. When M_t is close to zero, the conformal set \hat{C}_{t+1} expands significantly, as seen in (5). To mitigate this, we define the score function as

$$S(X, Y) = \frac{1}{p_f(Y|X)^{1/4}},$$

where X is an image, $Y \in 1, \dots, 62$ is a possible label, and $p_f(Y|X)$ is the probability assigned to Y by the pretrained model f . This choice ensures that lower predicted probabilities correspond to higher scores, aligning with the intuition that less certain predictions should be assigned greater importance. The exponent $1/4$ further sharpens the scores by amplifying the impact of particularly low-confidence predictions. We set the exponent to $1/4$ as it empirically yields favorable martingale dynamics, preventing M_t from collapsing too quickly to zero in practice. This choice is based on its consistent performance on our dataset, though a deeper theoretical understanding remains an open question.

We set the coverage level to $\alpha = 0.15$. The experiment is repeated 100 times, resampling both the calibration and final test sets at each iteration. Averaging over all runs, we obtain an empirical coverage of 0.94, exceeding the target level of $1 - \alpha = 0.85$.

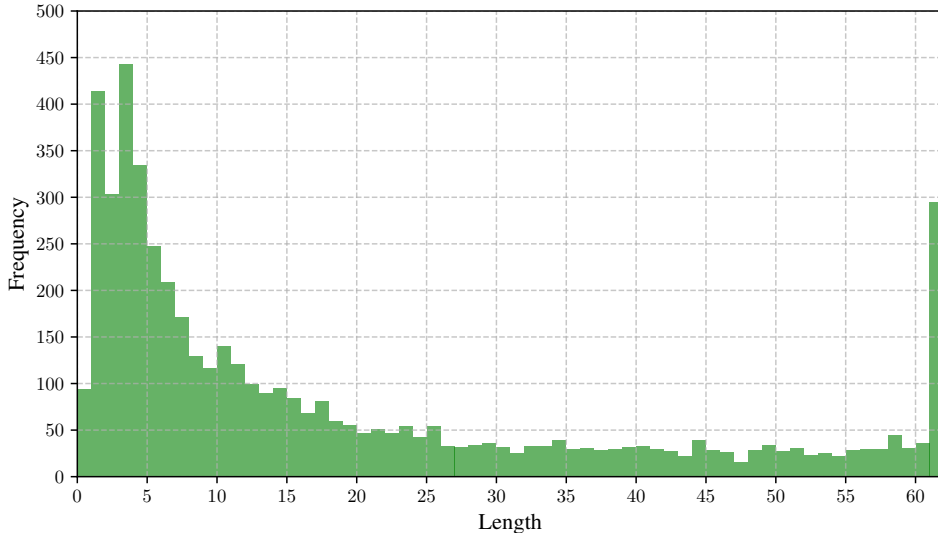


Figure 2: Histogram of conformal set sizes obtained across all $T = 50$ data batches and 100 iterations. The distribution illustrates the variability in set sizes, highlighting the proportion of informative and trivial sets.

This over-coverage can be attributed to several factors. First, Ville’s inequality is not necessarily tight, as is the case for Markov’s inequality. Second, the coverage guarantee is anytime-valid, meaning it must hold over an infinite sequence of batches. In contrast, our experiments are limited to $T = 50$ batches due to the finite amount of data available, which naturally leads to a higher observed coverage in practice.

This over-coverage is not necessarily a drawback, provided the conformal sets remain reasonably small and informative. Figure 2 shows the distribution of conformal set sizes across $T = 50$ data batches and 100 iterations. Most sets are relatively compact and convey meaningful information. However, a limitation of this method is that some sets can be trivial—in this case, those of size 62. Despite this, most remain informative and non-trivial, underscoring the approach’s practicality. It is worth noting that the method is model-agnostic and ensures coverage but does not control conformal set size; stronger models typically yield smaller sets. Appendix B provides a more detailed breakdown of conformal set sizes per batch, along with examples of batch anytime-valid conformal set sequences.

3 Fixed-Size Conformal Sets with Data-Dependent Coverage

Compared to p-variables, on which most existing conformal prediction methods are based, e-variables offer a more generalized form of coverage: they enable data-dependent coverage. This is why it is somewhat unfair to directly compare conformal p-prediction and conformal e-prediction, using a fixed coverage level α . E-variables provide a stronger guarantee, known as post-hoc validity, which allows for more flexible and adaptive inference. Further details on post-hoc validity and its connection to e-variables can be found in the following works: Wang and Ramdas [2022], Xu et al. [2024], Grünwald [2024], Ramdas and Wang [2024], Koning [2024]. Our discussion will specifically draw from the work by Koning [2024].

3.1 Theoretical framework

Definition 3.1 (Post-hoc p-variable, Definition 2 from Koning [2024]). We say that a nonnegative random variable P is a *post-hoc p-variable* if

$$\sup_{\tilde{\alpha}} \mathbb{E} \left[\frac{\mathbb{P}(P \leq \tilde{\alpha} \mid \tilde{\alpha})}{\tilde{\alpha}} \right] \leq 1,$$

where the supremum is over every random variable $\tilde{\alpha} \in (0, 1)$ that may not be independent from P .

P-variables are nonnegative random variables that satisfy the condition that their size distortion, $\frac{\mathbb{P}(P \leq \alpha)}{\alpha}$, for a given coverage level α , remains below 1. When the coverage is data-dependent, the size distortion itself becomes a random variable. The interpretation of Definition 3.1 of *post-hoc* p-variables is that certain distortions are permitted, provided they remain controlled in expectation. Remarkably, post-hoc p-variables are exactly the inverses of e-variables:

Theorem 3.2 (Theorem 2 from Koning [2024]). P is a post-hoc p-variable if and only if $\mathbb{E}[1/P] \leq 1$.

Therefore, conformal e-prediction methods yield data-dependent coverage guarantees, in the following sense:

Proposition 3.3. Consider a calibration set $\{(X_i, Y_i)\}_{i=1, \dots, n}$ and a test data point (X_{n+1}, Y_{n+1}) such that $(X_1, Y_1), \dots, (X_n, Y_n), (X_{n+1}, Y_{n+1})$ is exchangeable. Let $\tilde{\alpha}$ be any coverage level that may depend on this data. Then we have that:

$$\mathbb{E} \left[\frac{\mathbb{P}(Y_{n+1} \notin \hat{C}_n^{\tilde{\alpha}}(X_{n+1}) \mid \tilde{\alpha})}{\tilde{\alpha}} \right] \leq 1, \quad (6)$$

where

$$\hat{C}_n^{\tilde{\alpha}}(x) := \left\{ y : \frac{S(x, y)}{\frac{1}{n+1} (\sum_{i=1}^n S(X_i, Y_i) + S(x, y))} < 1/\tilde{\alpha} \right\}. \quad (7)$$

Proof. Recall that the random variable

$$E = \frac{S(X_{n+1}, Y_{n+1})}{\frac{1}{n+1} \sum_{i=1}^{n+1} S(X_i, Y_i)}$$

defined in Equation (4) is an e-variable [see Balinsky and Balinsky, 2024]. Therefore, by Theorem 3.2, $P = 1/E$ is a post-hoc p-variable. The only thing left to see is that

$$\begin{aligned} P \leq \tilde{\alpha} &\iff E \geq 1/\tilde{\alpha} \\ &\iff \frac{S(X_{n+1}, Y_{n+1})}{\frac{1}{n+1} \sum_{i=1}^{n+1} S(X_i, Y_i)} \geq 1/\tilde{\alpha} \\ &\iff Y_{n+1} \notin \hat{C}_n^{\tilde{\alpha}}(X_{n+1}) \end{aligned}$$

by definition of $\hat{C}_n^{\tilde{\alpha}}$. □

In practice, practitioners can define a random variable $\tilde{\alpha}$ that depends only on the observed data $\{(X_i, Y_i)\}_{i=1, \dots, n}$ and X_{n+1} , but not on Y_{n+1} . When $\tilde{\alpha} = \alpha$ is a constant that does not depend on data, the guarantee (6) can be rewritten as

$$\mathbb{P}(Y_{n+1} \notin \hat{C}_n^{\alpha}(X_{n+1})) \leq \alpha,$$

which is exactly (1). More generally, when $\tilde{\alpha}$ is well-concentrated around its mean, we can use a first-order Taylor expansion to obtain:

$$\mathbb{E} \left[\frac{\mathbb{P}(Y_{n+1} \notin \hat{C}_n^{\tilde{\alpha}}(X_{n+1}) \mid \tilde{\alpha})}{\tilde{\alpha}} \right] \approx \frac{\mathbb{E}[\mathbb{P}(Y_{n+1} \notin \hat{C}_n^{\tilde{\alpha}}(X_{n+1}) \mid \tilde{\alpha})]}{\mathbb{E}[\tilde{\alpha}]} = \frac{\mathbb{P}(Y_{n+1} \notin \hat{C}_n^{\tilde{\alpha}}(X_{n+1}))}{\mathbb{E}[\tilde{\alpha}]}$$

and derive meaningful guarantees of the form:

$$\mathbb{P}(Y_{n+1} \in \hat{C}_n^{\tilde{\alpha}}(X_{n+1})) \geq 1 - \mathbb{E}[\tilde{\alpha}]. \quad (8)$$

Since $\mathbb{E}[\tilde{\alpha}]$ is not known in practice, we can use concentration inequalities to obtain useful guarantees. For example, assume that $\tilde{\alpha}$ is σ -sub-Gaussian. Then, $\tilde{\alpha}$ satisfies the deviation inequality $\mathbb{P}(\tilde{\alpha} \leq \mathbb{E}[\tilde{\alpha}] - t) \leq \exp\left(-\frac{t^2}{2\sigma^2}\right)$ for all $t \in \mathbb{R}$, and we obtain guarantees of the form:

$$\mathbb{P}(Y_{n+1} \in \hat{C}_n^{\tilde{\alpha}}(X_{n+1})) \geq 1 - \tilde{\alpha} - \sigma\sqrt{2\log(1/\delta)}, \quad (9)$$

with probability at least $1 - \delta$.

Therefore, e-variables can be utilized to derive conformal prediction guarantees that adapt to the data. This enables, for instance, the construction of conformal sets with a specified size. In the classification setting, suppose we aim to obtain conformal sets of size (at most) C . Traditional conformal prediction methods do not allow for such control. However, by leveraging e-variables, we can define

$$\tilde{\alpha} := \inf \left\{ \alpha \in (0, 1) : \# \left\{ y : \frac{S(X_{n+1}, y)}{\frac{1}{n+1} (\sum_{i=1}^n S(X_i, Y_i) + S(X_{n+1}, y))} < 1/\alpha \right\} \leq C \right\} \quad (10)$$

and establish guarantees of the form (6), (8), and (9), while ensuring that the conformal sets are of size (at most) C . This approach enables practitioners to make informed decisions based on the observed $\tilde{\alpha}$. It is only feasible with e-variables, as they provide post-hoc guarantees in contrast with the fixed-level α guarantees of conformal p-prediction.

3.2 Experiments

We use the same dataset and the same pretrained model f as in Section 2. For our experiments, we randomly sample a calibration set of size 2000 from the test set and select a test data point (X_{n+1}, Y_{n+1}) from the remaining data points. Our goal is to obtain conformal sets of size (at most) C , with a data-dependent coverage. To achieve this, we determine $\tilde{\alpha}$ based on Equation (10), that depends on the calibration set and the test feature X_{n+1} . For ease of implementation, we define a discrete set of candidate values: $\mathbb{A} = \{0.01, 0.02, 0.03, \dots, 0.29, 0.3\}$, and select

$$\tilde{\alpha} := \inf \left\{ \alpha \in \mathbb{A} : \# \left\{ y : \frac{S(X_{n+1}, y)}{\frac{1}{n+1} (\sum_{i=1}^n S(X_i, Y_i) + S(X_{n+1}, y))} < 1/\alpha \right\} \leq C \right\}. \quad (11)$$

The score function we use is the cross-entropy, formally defined in Equation (2). We average the results over 100 iterations, each with a randomly sampled calibration set. In each iteration, we compute a data-dependent coverage level $\tilde{\alpha}$ and construct conformal sets of size (at most) C using (7). The values of $\tilde{\alpha}$ for $C = 3$ and $C = 5$ are shown in Figure 3. Empirically, we observe that inequality (8) holds, supporting the first-order Taylor approximation used in our method to derive guarantees (8) and (9). We provide examples of the obtained conformal sets and illustrate how their size evolves as α varies in Appendix C.

This method introduces a conceptual inversion of conformal prediction: instead of fixing a coverage level and potentially obtaining conformal sets of impractical size, we set a maximum conformal set size threshold C up front. We then obtain guarantees for an observed coverage level $\tilde{\alpha}$, which is data-dependent and adaptive in the sense that it varies with the test feature X_{n+1} . This allows practitioners to make informed decisions based on the observed coverage while ensuring that the resulting conformal sets remain meaningful.

We present a sample result in Figure 4. Specifically, this sample corresponds to a random draw of the calibration set and test data point. We construct the associated conformal set for each $\alpha \in \mathbb{A}$ using (11).

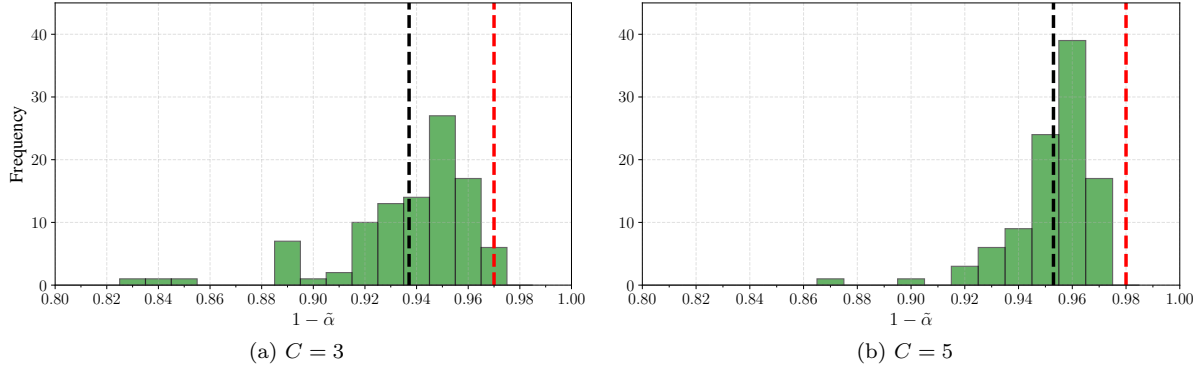


Figure 3: Histogram of $1 - \tilde{\alpha}$ for $C = 3$ and $C = 5$, computed across 100 iterations. The black dashed line represents the expected coverage level, $1 - \mathbb{E}[\tilde{\alpha}]$, while the red dashed line corresponds to the empirical coverage probability, $\mathbb{P}(Y_{n+1} \in \hat{C}_n^{\tilde{\alpha}}(X_{n+1}))$, both estimated over the 100 iterations.

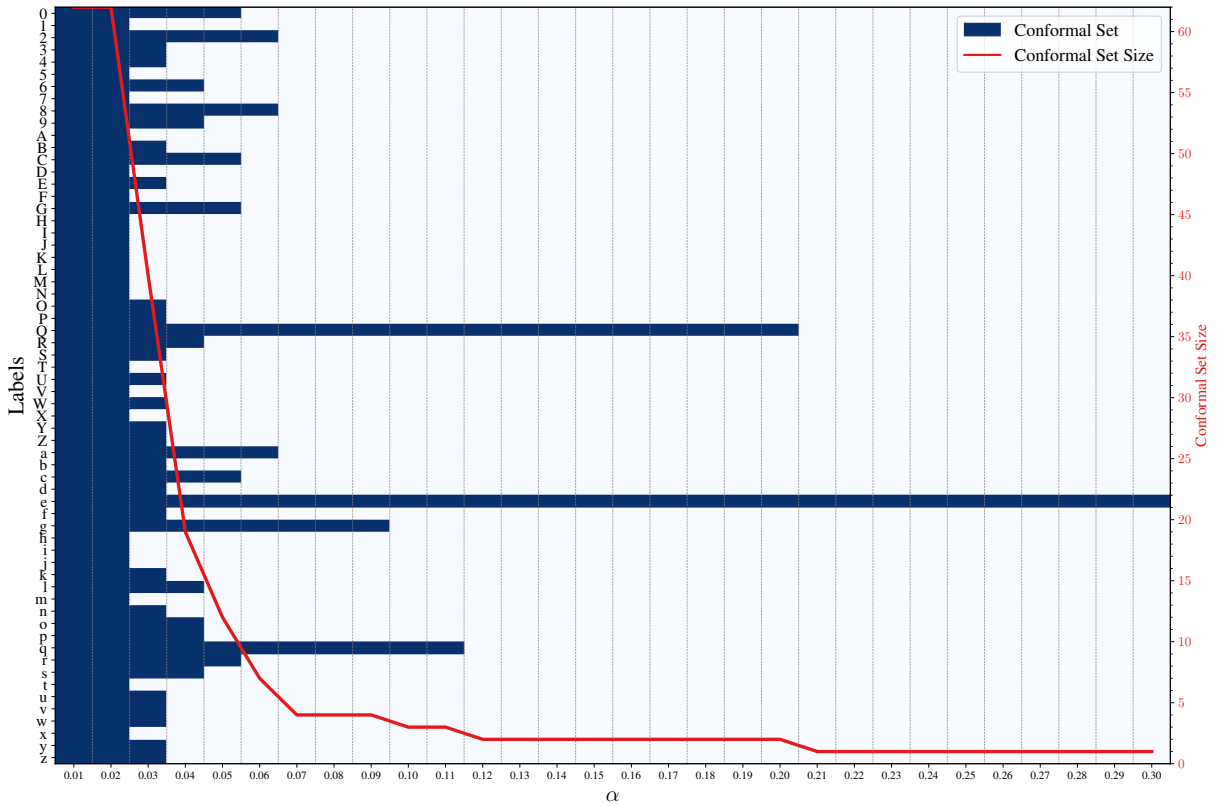


Figure 4: Example of conformal sets obtained with varying $\tilde{\alpha}$.

The x-axis represents the different values of α , while the y-axis corresponds to the possible labels. For each α , the conformal sets are shown as dark blue cells. Additionally, we plot in red the size of the conformal sets as a function of α .

The method allows us to select $\tilde{\alpha}$ based on the calibration data and test image X_{n+1} . For instance, if we aim to obtain conformal sets with a size (at most) $C = 5$, applying Equation (10) yields $\tilde{\alpha} = 0.07$ in the example of Figure 4. We provide additional sample results in Appendix C.

4 Conformal Prediction under Ambiguous Ground Truth

The conformal e-prediction framework also provides valid guarantees in Monte Carlo conformal prediction, a problem introduced by Stutz et al. [2023]. When the ground truth is ambiguous and $m \geq 1$ labels

are sampled from $\mathbb{P}_{Y|X_i}$ for each feature X_i , it is possible to account for all m labels while obtaining conformal prediction guarantees. Instead of selecting a single label and discarding the rest to enforce exchangeable data, an approach that leverages all m labels reduces variability in the conformal prediction guarantees. [Stutz et al. \[2023\]](#) propose a method to achieve this based on a classical result by [Rüschendorf \[1982\]](#) and later independently established by [Meng \[1994\]](#) on averaging arbitrary p-variables, which yields a p-variable up to a factor of 2. Consequently, this approach ensures a coverage level of $1 - 2\alpha$, with this factor of 2 being theoretically unavoidable. Constructing conformal sets using e-variables, however, guarantees a theoretical coverage of at least $1 - \alpha$.

4.1 Monte Carlo conformal p-prediction [[Stutz et al., 2023](#)]

We will write $S_i^j := S(X_i, Y_i^j)$ for $i = 1, \dots, n$ and $j = 1, \dots, m$. We will also write $S_{n+1} := S(X_{n+1}, Y_{n+1})$. We reformulate the main result by [Stutz et al. \[2023\]](#), adapted for negatively-oriented scores instead of positively-oriented ones, which is the primary focus of their paper.

Theorem 4.1. *The following conformal set:*

$$\hat{C}_n(x) := \left\{ y : \frac{1}{mn} \sum_{j=1}^m \sum_{i=1}^n \mathbb{1}_{\{S_i^j \leq S(x, y)\}} \leq \frac{\lceil m(1 - \alpha)(n + 1) \rceil - 1}{mn} \right\} \quad (12)$$

$$= \left\{ y : S(x, y) \leq \text{quantile} \left(\frac{\lceil m(1 - \alpha)(n + 1) \rceil - 1}{mn}; \frac{1}{mn} \sum_{j=1}^m \sum_{i=1}^n \delta_{S_i^j} \right) \right\} \quad (13)$$

with δ_z denoting a point mass at z , satisfies property (1) with coverage $1 - 2\alpha$ instead of $1 - \alpha$:

$$\mathbb{P}(Y_{n+1} \in \hat{C}_n(X_{n+1})) \geq 1 - 2\alpha.$$

Proof. Let $\alpha \in (0, 1)$. We have:

$$\begin{aligned} \frac{1}{mn} \sum_{j=1}^m \sum_{i=1}^n \mathbb{1}_{\{S_i^j \leq S_{n+1}\}} &\leq \frac{\lceil m(1 - \alpha)(n + 1) \rceil - 1}{mn} \Leftrightarrow \sum_{j=1}^m \sum_{i=1}^n \mathbb{1}_{\{S_i^j \leq S_{n+1}\}} \leq \lceil m(1 - \alpha)(n + 1) \rceil - 1 \\ &\Leftrightarrow \sum_{j=1}^m \sum_{i=1}^n \mathbb{1}_{\{S_i^j \leq S_{n+1}\}} < m(1 - \alpha)(n + 1) \\ &\Leftrightarrow mn - \sum_{j=1}^m \sum_{i=1}^n \mathbb{1}_{\{S_i^j > S_{n+1}\}} < m(1 - \alpha)(n + 1) \\ &\Leftrightarrow \sum_{j=1}^m \sum_{i=1}^n \mathbb{1}_{\{S_i^j > S_{n+1}\}} > mn - m(1 - \alpha)(n + 1) \\ &\Leftrightarrow \frac{1}{m} \sum_{j=1}^m \frac{\sum_{i=1}^n \mathbb{1}_{\{S_i^j > S_{n+1}\}} + 1}{n + 1} > \alpha, \end{aligned}$$

and we will show that the last inequality holds with probability $\geq 1 - 2\alpha$. First, see that for a fixed $j = 1, \dots, m$, the random variables $S_1^j, \dots, S_n^j, S_{n+1}$ are exchangeable. Therefore, the random variables

$$P_j := \frac{\sum_{i=1}^n \mathbb{1}_{\{S_i^j > S_{n+1}\}} + 1}{n + 1}$$

are p-variables (see Lemma A.4 in Appendix A). Let $\bar{P} := \frac{1}{m} \sum_{j=1}^m P_j$ be the arithmetic mean of these p-variables. Then, by [Rüschendorf \[1982\]](#), [Meng \[1994\]](#), $2\bar{P}$ is a p-variable:

$$\forall \alpha \in (0, 1), \mathbb{P}(2\bar{P} \leq \alpha) \leq \alpha \iff \forall \alpha \in (0, 1), \mathbb{P}(\bar{P} > \alpha) \geq 1 - 2\alpha,$$

which concludes the proof. \square

Even if there exist other ways of combining p-variables (see, for example, [Vovk and Wang \[2020\]](#)), the advantage of averaging p-variables using the arithmetic mean is that it preserves the interpretation of

conformal sets as quantiles of the empirical cumulative distribution function. However, this approach comes at the cost of achieving coverage of $1 - 2\alpha$ instead of $1 - \alpha$. We now show that moving beyond the traditional framework of conformal p-prediction based on rank-based statistics and instead leveraging e-variables yields conformal sets with coverage $1 - \alpha$.

4.2 Monte Carlo conformal e-prediction

E-variables are particularly convenient to handle. Specifically, it is evident that if E_1, \dots, E_m are e-variables, then their arithmetic mean:

$$\bar{E} := \frac{1}{m} \sum_{j=1}^m E_j \quad (14)$$

is also an e-variable. We keep the same notation as before. For each $j \in \{1, \dots, m\}$, the random variables $S_1^j, \dots, S_n^j, S_{n+1}$ are exchangeable so the random variables

$$E_j := \frac{S_{n+1}}{\frac{1}{n+1}(\sum_{i=1}^n S_i^j + S_{n+1})}$$

are e-variables. By applying Markov’s inequality to \bar{E} defined in (14), we derive a new way to construct conformal sets in Monte Carlo conformal prediction:

Theorem 4.2. *The following conformal set:*

$$\hat{C}_n(x) := \left\{ y : \frac{1}{m} \sum_{j=1}^m \frac{S(x, y)}{\frac{1}{n+1}(\sum_{i=1}^n S(X_i, Y_i^j) + S(x, y))} < 1/\alpha \right\} \quad (15)$$

satisfies property (1).

One possible interpretation is as follows: assume one of the m experts, denoted j_0 , predicts that $E_{j_0} \geq 1/\alpha$, meaning that the expert believes that the test point’s score is abnormally high. This expert might be incorrect. The conformal set (15) smoothes the predictions by averaging all the predictions from expert j_0 and the remaining $m - 1$ experts.

4.3 Experiments

In this section, we base our experiments on the CIFAR-10 dataset [Krizhevsky, 2009]. CIFAR-10 is a widely used benchmark dataset in computer vision, consisting of 60,000 color images of size 32×32 pixels, categorized into 10 classes: airplane, automobile, bird, cat, deer, dog, frog, horse, ship, and truck. The dataset is divided into 50,000 training images and 10,000 test images, with an equal number of samples per class.

We train an EfficientNetB0 model [Tan and Le, 2019] using cross-entropy loss, optimized with stochastic gradient descent. The learning rate is initialized at 0.1 and adjusted with a cosine annealing schedule. Training is conducted over 100 epochs with a batch size of 512, incorporating data augmentation techniques. The resulting classifier f achieves an accuracy of 98.6% on the training set and 91.1% on the test set. Once trained, we treat f as a black-box model for generating predictions.

The Monte Carlo conformal prediction method is particularly relevant in cases where the ground truth is ambiguous. For this reason, we use the CIFAR-10H dataset [Peterson et al., 2019], which extends CIFAR-10 by incorporating human-labeled annotations for the 10,000 images of the test set. For each image, human annotators provide class labels, offering an additional source of ground truth that can be used to assess model performance in comparison to human judgment. This human-annotated version of CIFAR-10 is particularly useful for tasks where model uncertainty is of interest.

We filter the test dataset to include only ambiguous examples. Specifically, we retain only images with label distributions where at least two labels have a probability ≥ 0.1 . This results in a filtered test dataset of size 857. This dataset is then divided into a calibration set comprising 30% of the data and a final test set with the remaining 70%.

On the filtered test dataset, the model f achieves an accuracy of 71.41%. Similar to Stutz et al. [2023], which selects a coverage matching the accuracy of the pretrained model, we set $\alpha = 0.3$ to stay comparable with the base model. We use cross-entropy (2) as the score function S .

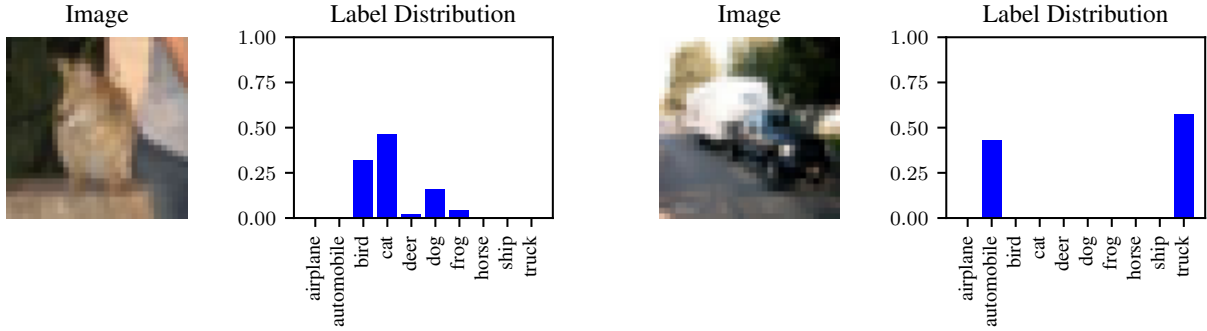


Figure 5: Some images from CIFAR-10H with ambiguous ground truth, along with their label distributions.

Figures 6 and 7 show the coverage and conformal set size obtained with conformal e-prediction and conformal p-prediction respectively, comparing $m = 1$ and $m = 20$ experts across 200 random splits between the calibration and final test sets. We overlap the histograms for $m = 1$ and $m = 20$ using a fixed bin width. Increasing the number of experts m reduces the variability in coverage and conformal set sizes observed across calibration and test splits, for both methods. This is consistent with the observation of [Stutz et al. \[2023\]](#) in the case of conformal p-prediction. The conformal sets obtained with e-variables exhibit larger coverage than the target $1 - \alpha$ and are reasonably larger than the conformal sets obtained with conformal p-prediction. We also note that although Monte Carlo conformal p-prediction has a theoretical coverage of $1 - 2\alpha$, we empirically observe a coverage of $1 - \alpha$, consistent with the empirical findings of [Stutz et al. \[2023\]](#).

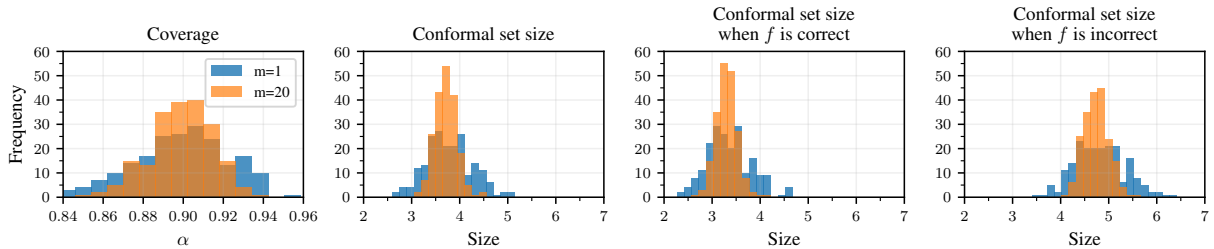


Figure 6: Comparison of coverage and conformal set sizes when using e-variables in Monte Carlo conformal prediction with $m = 1$ or $m = 20$ experts, with $\alpha = 0.3$, from [Theorem 15](#).

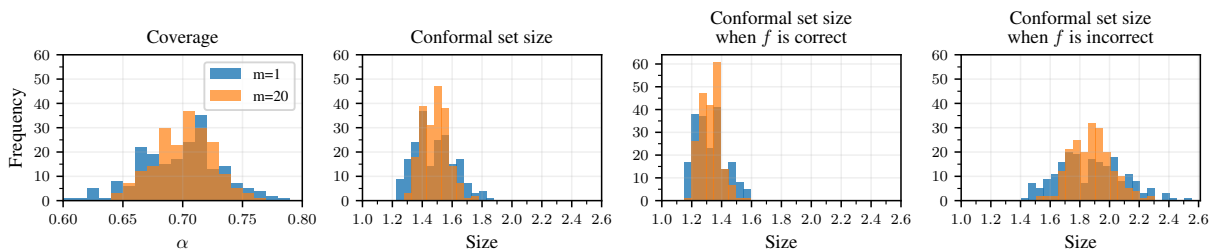


Figure 7: Comparison of coverage and conformal set sizes when using p-variables in Monte Carlo conformal prediction with $m = 1$ or $m = 20$ experts, with $\alpha = 0.3$, from [Theorem 12](#).

Note that to achieve a theoretical coverage guarantee of 0.70 in Monte Carlo conformal p-prediction, one can set $\alpha = 0.15$, as this method theoretically ensures a coverage of $1 - 2\alpha$ rather than $1 - \alpha$. Empirically, this would yield conformal sets with a coverage of 0.85, almost matching those obtained in Monte Carlo conformal e-prediction, which achieve an empirical coverage of approximately 0.90.

Monte Carlo conformal e-prediction is a theoretical alternative to Monte Carlo conformal p-prediction, providing a theoretical coverage guarantee of $1 - \alpha$. However, in practice, Monte Carlo conformal p-prediction also achieves an empirical coverage of $1 - \alpha$ rather than the theoretically guaranteed $1 - 2\alpha$, and seems to achieve higher-quality predictions. The reason behind this discrepancy remains unclear and is still an open problem.

5 Conclusion

In this work, we highlighted the flexibility of conformal e-prediction for uncertainty quantification. While traditional conformal p-prediction will continue to provide an important tool, in particular in standard statistical settings where data are exchangeable and a fixed coverage level α is employed, conformal e-prediction provides an appealing alternative for more complex scenarios, particularly when data are not fully exchangeable. We exhibited this flexibility in three settings where e-variables yield theoretically well-grounded conformal prediction guarantees: batch anytime-valid conformal prediction, fixed-size conformal sets with data-dependent coverage, and conformal prediction under ambiguous ground truth. These results highlight the potential of conformal e-prediction as a flexible tool for uncertainty quantification for complex problems in machine learning.

We believe there is much more to explore in conformal e-prediction. One ongoing challenge is the choice of the score function, which plays a crucial role in determining the size of conformal sets. Selecting an optimal score function is particularly important in settings like batch anytime-valid prediction, where it directly impacts the dynamics of the martingale.

Beyond this, further investigation into the applications introduced in this paper could yield valuable insights. In batch anytime-valid conformal prediction, an interesting question is whether we can use alternatives to Ville’s inequality that provide tighter bounds. While Ville’s inequality holds for supermartingales, we could explore inequalities that apply to martingales as well, given that M_t introduced in Theorem 2.5 is not only a supermartingale but also a martingale. Another avenue is the choice of the martingale itself—could different constructions lead to stronger results? In particular, it would be interesting to investigate whether incorporating λ_t terms that depend on the data up to time $t - 1$, as explained in Remark 2.7, could lead to improved performance.

Acknowledgements

The authors would like to thank Eugène Berta, Nabil Boukir, Sacha Braun, Aymeric Capitaine, Mahmoud Hegazy, Antoine Scheid, and Ian Waudby-Smith for their constructive reflections on conformal prediction and e-values, which have provided valuable insights.

Funded by the European Union (ERC-2022-SYG-OCEAN-101071601). Views and opinions expressed are however those of the author(s) only and do not necessarily reflect those of the European Union or the European Research Council Executive Agency. Neither the European Union nor the granting authority can be held responsible for them.

This publication is part of the Chair “Markets and Learning,” supported by Air Liquide, BNP PARIBAS ASSET MANAGEMENT Europe, EDF, Orange and SNCF, sponsors of the Inria Foundation.

This work has also received support from the French government, managed by the National Research Agency, under the France 2030 program with the reference “PR[AI]RIE-PSAI” (ANR-23-IACL-0008).

References

- Anastasios N. Angelopoulos and Stephen Bates. Conformal prediction: A gentle introduction. *Found. Trends Mach. Learn.*, 16(4):494–591, 2023.
- Anastasios N. Angelopoulos, Rina Foygel Barber, and Stephen Bates. Theoretical foundations of conformal prediction. *arXiv preprint arXiv:2411.11824*, 2024.
- Anastasios Nikolas Angelopoulos, Stephen Bates, Michael Jordan, and Jitendra Malik. Uncertainty sets for image classifiers using conformal prediction. In *International Conference on Learning Representations*, 2021.
- Vineeth Balasubramanian, Shen-Shyang Ho, and Vladimir Vovk. *Conformal Prediction for Reliable Machine Learning: Theory, Adaptations and Applications*. Morgan Kaufmann Publishers Inc., 2014.
- Alexander A. Balinsky and Alexander D. Balinsky. Enhancing conformal prediction using e-test statistics. *arXiv preprint arXiv:2403.19082*, 2024.

- Sebastian Caldas, Peter Wu, Tian Li, Jakub Konečný, H. Brendan McMahan, Virginia Smith, and Ameet Talwalkar. LEAF: A benchmark for federated settings. *arXiv preprint arXiv:1812.01097*, 2018.
- Gregory Cohen, Saeed Afshar, Jonathan Tapson, and André van Schaik. EMNIST: Extending MNIST to handwritten letters. In *International Joint Conference on Neural Networks (IJCNN)*, pages 2921–2926, 2017.
- Thomas M. Cover. Universal portfolios. *Mathematical Finance*, page 1–29, 1991.
- Thomas M. Cover and Erik Ordentlich. Universal portfolios with side information. *IEEE Transactions on Information Theory*, 42(2):348–363, 1996.
- Joseph L. Doob. *Stochastic Processes*. Wiley, 1953.
- Isaac Gibbs, John J. Cherian, and Emmanuel Candès. Conformal prediction with conditional guarantees. *arXiv preprint arXiv:2305.12616*, 2024.
- Peter D. Grünwald. Beyond Neyman-Pearson: E-values enable hypothesis testing with a data-driven alpha. *Proceedings of the National Academy of Sciences*, 121(39):e2302098121, 2024.
- Steven R. Howard, Aaditya Ramdas, Jon McAuliffe, and Jasjeet Sekhon. Time-uniform, nonparametric, nonasymptotic confidence sequences. *The Annals of Statistics*, 49(2):1055–1080, 2021.
- Kexin Huang, Ying Jin, Emmanuel Candès, and Jure Leskovec. Uncertainty quantification over graph with conformalized graph neural networks. In *Proceedings of the International Conference on Neural Information Processing Systems*, 2023.
- Ying Jin and Emmanuel Candès. Selection by prediction with conformal p-values. *J. Mach. Learn. Res.*, 24(1), 2023.
- Christopher Jung, Georgy Noarov, Ramya Ramalingam, and Aaron Roth. Batch multivald conformal prediction. In *International Conference on Learning Representations*, 2023.
- Nick W. Koning. Post-hoc α hypothesis testing and the post-hoc p-value. *arXiv preprint arXiv:2312.08040*, 2024.
- Alex Krizhevsky. Learning multiple layers of features from tiny images. Technical report, University of Toronto, 2009.
- Yann LeCun. The MNIST database of handwritten digits. <http://yann.lecun.com/exdb/mnist/>, 1998.
- Yann LeCun, Léon Bottou, Yoshua Bengio, and Patrick Haffner. Gradient-based learning applied to document recognition. *Proceedings of the IEEE*, 86(11):2278–2324, 1998.
- Xiao-Li Meng. Posterior predictive p-values. *The Annals of Statistics*, 22(3):1142–1160, 1994.
- Francesco Orabona and Kwang-Sung Jun. Tight concentrations and confidence sequences from the regret of universal portfolio. *IEEE Transactions on Information Theory*, 2023.
- Harris Papadopoulos, Kostas Proedrou, Vladimir Vovk, and Alexander Gammerman. Inductive confidence machines for regression. In *European Conference on Machine Learning*, 2002.
- Joshua Peterson, Ruairidh Battleday, Thomas Griffiths, and Olga Russakovsky. Human uncertainty makes classification more robust. In *IEEE/CVF International Conference on Computer Vision (ICCV)*, pages 9616–9625, 2019.
- Aaditya Ramdas and Ruodu Wang. Hypothesis testing with e-values. *arXiv preprint arXiv:2410.23614*, 2024.
- Yaniv Romano, Evan Patterson, and Emmanuel Candès. Conformalized quantile regression. In *Advances in Neural Information Processing Systems*, 2019.
- Yaniv Romano, Matteo Sesia, and Emmanuel Candès. Classification with valid and adaptive coverage. In *Advances in Neural Information Processing Systems*, 2020.

- J. Jon Ryu and Alankrita Bhatt. On confidence sequences for bounded random processes via universal gambling strategies. *IEEE Trans. Inf. Theor.*, 70(10):7143–7161, 2024.
- Ludger Rüschendorf. Random variables with maximum sums. *Advances in Applied Probability*, 14(3): 623–632, 1982.
- Mauricio Sadinle, Jing Lei, and Larry Wasserman. Least ambiguous set-valued classifiers with bounded error levels. *Journal of the American Statistical Association*, 114(525):223–234, 2019.
- David Stutz, Krishnamurthy Dvijotham, Ali Taylan Cemgil, and Arnaud Doucet. Learning optimal conformal classifiers. In *International Conference on Learning Representations*, 2022.
- David Stutz, Abhijit Guha Roy, Tatiana Matejovicova, Patricia Strachan, Ali Taylan Cemgil, and Arnaud Doucet. Conformal prediction under ambiguous ground truth. *Transactions on Machine Learning Research*, 2023.
- Mingxing Tan and Quoc Le. EfficientNet: Rethinking model scaling for convolutional neural networks. In *International Conference on Machine Learning*, 2019.
- Jean Ville. *Étude Critique de la Notion de Collectif*. Université de Paris, 1939.
- Vladimir Vovk. Aggregating strategies. In *Proceedings of the Annual Workshop on Computational Learning Theory*, page 371–386, 1990.
- Vladimir Vovk. Conformal e-prediction. *arXiv preprint arXiv:2001.05989*, 2024.
- Vladimir Vovk and Ruodu Wang. Combining p-values via averaging. *Biometrika*, 107(4):791–808, 2020.
- Vladimir Vovk and Ruodu Wang. E-values: Calibration, combination and applications. *The Annals of Statistics*, 49, 2021.
- Vladimir Vovk and Christopher Watkins. Universal portfolio selection. In *Proceedings of the Annual Conference on Computational Learning Theory*, page 12–23, 1998.
- Vladimir Vovk, Alex Gammerman, and Glenn Shafer. *Algorithmic Learning in a Random World*. Springer-Verlag, 2005.
- Qiuqi Wang, Ruodu Wang, and Johanna Ziegel. E-backtesting. *arXiv preprint arXiv:2209.00991*, 2024.
- Ruodu Wang and Aaditya Ramdas. False discovery rate control with e-values. *Journal of the Royal Statistical Society Series B*, 84(3):822–852, 2022.
- Ian Waudby-Smith and Aaditya Ramdas. Estimating means of bounded random variables by betting. *Journal of the Royal Statistical Society Series B: Statistical Methodology*, 86, 2023.
- David Williams. *Probability with Martingales*. Cambridge University Press, 1991.
- Ziyu Xu, Ruodu Wang, and Aaditya Ramdas. Post-selection inference for e-value based confidence intervals. *Electronic Journal of Statistics*, 18(1):2292 – 2338, 2024.

A Background on Conformal p-Prediction

In this appendix, we review key concepts in conformal (p-)prediction, introduced by Vovk et al. [2005], to provide a comprehensive foundation. In our work, we focus on split conformal prediction [Papadopoulos et al., 2002], and we explore the applications of conformal prediction methods in machine learning, a broad and active area of research (see, for example, Balasubramanian et al. [2014], Romano et al. [2019], Sadinle et al. [2019], Romano et al. [2020], Angelopoulos et al. [2021], Stutz et al. [2022], Huang et al. [2023]). For a recent overview of conformal prediction, we refer the reader to Angelopoulos and Bates [2023] and Angelopoulos et al. [2024].

Definition A.1 (Exchangeability). Random variables S_1, \dots, S_n are said to be *exchangeable* if: for any permutation $\sigma \in \mathfrak{S}_n$, the distribution of the random vector (S_1, \dots, S_n) is the same as that of $(S_{\sigma(1)}, \dots, S_{\sigma(n)})$.

Exchangeability is a weaker property than the common notion of independent and identically distributed (i.i.d.) random variables. The fundamental idea of conformal p-prediction is based on a simple observation: since the scores $S_i = S(X_i, Y_i)$ for $i = 1, \dots, n, n+1$, are exchangeable, their order⁵ follows a uniform distribution. In particular, this implies that:

$$\mathbb{P}(S_{n+1} \leq \text{the } \lceil (1-\alpha)(n+1) \rceil \text{ smallest of } S_1, \dots, S_{n+1}) \geq 1-\alpha,$$

and it turns out that we can rewrite the inequality above as

$$\mathbb{P}(S_{n+1} \leq \text{the } \lceil (1-\alpha)(n+1) \rceil \text{ smallest of } S_1, \dots, S_n) \geq 1-\alpha$$

by artificially defining the $n+1$ smallest value among S_1, \dots, S_n to be $+\infty$. Therefore, the following conformal set:

$$\hat{C}_n(x) := \{y : S(x, y) \leq \text{the } \lceil (1-\alpha)(n+1) \rceil \text{ smallest of } S(X_1, Y_1), \dots, S(X_n, Y_n)\} \quad (16)$$

effectively satisfies (1). Note that we can rewrite \hat{C}_n using the empirical cumulative distribution function of $S(X_1, Y_1), \dots, S(X_n, Y_n)$ as follows:

$$\hat{C}_n(x) = \left\{ y : \frac{1}{n} \sum_{i=1}^n \mathbb{1}_{\{S(X_i, Y_i) \leq S(x, y)\}} \leq \frac{\lceil (1-\alpha)(n+1) \rceil}{n} \right\}. \quad (17)$$

\hat{C}_n is also commonly rewritten as:

$$\hat{C}_n(x) = \left\{ y : S(x, y) \leq \text{quantile} \left(\frac{\lceil (1-\alpha)(n+1) \rceil}{n}; \frac{1}{n} \sum_{i=1}^n \delta_{S(X_i, Y_i)} \right) \right\}, \quad (18)$$

where the quantile function returns $+\infty$ when the input is ≥ 1 . The interpretation of (16), (17), and (18) is that, with high probability, the test value $S(X_{n+1}, Y_{n+1})$ cannot significantly exceed the values $S(X_i, Y_i)$ in the calibration set.

The formulation (17) can be reinterpreted through the lens of p-variables. We recall the definition of p-variables:

Definition A.2 (p-variable). A *p-variable* P is a nonnegative random variable that satisfies

$$\mathbb{P}(P \leq \alpha) \leq \alpha$$

for all $\alpha \in (0, 1)$.

Remark A.3. Equivalently, a nonnegative random variable P is a p-variable if, for all $\alpha \in (0, 1)$, its *size distortion* $\mathbb{P}(P \leq \alpha)/\alpha$ at level α is at most 1. This equivalent definition is especially meaningful in the discussion of Section 3, where we leverage the post-hoc statistical properties that e-variables provide, in contrast to p-variables.

⁵The notion of order is well-defined if we assume that the S_i are almost surely distinct. Otherwise, we can use an appropriate random tie-breaking rule and the results still hold.

Lemma A.4 (Reformulation of (17) with p-variables). *The following random variable:*

$$\frac{\sum_{i=1}^n \mathbb{1}_{\{S_i > S_{n+1}\}} + 1}{n+1}$$

is a p-variable.

Proof. Let $\alpha \in (0, 1)$. We want to show that $\mathbb{P}\left(\frac{\sum_{i=1}^n \mathbb{1}_{\{S_i > S_{n+1}\}} + 1}{n+1} \leq \alpha\right) \leq \alpha$, which is equivalent to $\mathbb{P}\left(\frac{\sum_{i=1}^n \mathbb{1}_{\{S_i > S_{n+1}\}} + 1}{n+1} > \alpha\right) \geq 1 - \alpha$. Note that:

$$\begin{aligned} \frac{\sum_{i=1}^n \mathbb{1}_{\{S_i > S_{n+1}\}} + 1}{n+1} > \alpha &\Leftrightarrow \sum_{i=1}^n \mathbb{1}_{\{S_i > S_{n+1}\}} > \alpha(n+1) - 1 \\ &\Leftrightarrow n - \sum_{i=1}^n \mathbb{1}_{\{S_i \leq S_{n+1}\}} > \alpha(n+1) - 1 \\ &\Leftrightarrow \sum_{i=1}^n \mathbb{1}_{\{S_i \leq S_{n+1}\}} < (1-\alpha)(n+1) \\ &\Leftrightarrow \sum_{i=1}^n \mathbb{1}_{\{S_i \leq S_{n+1}\}} < \lceil (1-\alpha)(n+1) \rceil \quad \text{since } \sum_{i=1}^n \mathbb{1}_{\{S_i \leq S_{n+1}\}} \in \mathbb{N} \\ &\Leftrightarrow \frac{1}{n} \sum_{i=1}^n \mathbb{1}_{\{S_i \leq S_{n+1}\}} < \frac{\lceil (1-\alpha)(n+1) \rceil}{n}, \end{aligned}$$

and this last event indeed occurs with probability $\geq 1 - \alpha$ since the conformal set (17) satisfies Property (1), which concludes the proof. \square

Conformal p-prediction not only ensures that $\mathbb{P}(Y_{n+1} \in \hat{C}_n(X_{n+1})) \geq 1 - \alpha$, but also guarantees that $\mathbb{P}(Y_{n+1} \in \hat{C}_n(X_{n+1})) \leq 1 - \alpha + \frac{1}{n+1}$, provided there are almost surely no ties between the scores.

B Details on Section 2

B.1 Network architecture and training details

The model f consists of two convolutional layers followed by three fully connected layers. The first convolutional layer applies 6 filters of size 5×5 to the input grayscale images, followed by a ReLU activation and 2×2 max pooling. The second convolutional layer applies 16 filters of size 5×5 , followed by another ReLU activation and 2×2 max pooling. The output of the second convolutional layer is flattened and passed through three fully connected layers: 120 neurons with ReLU activation, 84 neurons with ReLU activation, and finally 62 output neurons corresponding to the number of classes. The model is trained using cross-entropy loss and SGD with a learning rate of 0.1 for 100 epochs, using cosine annealing and a batch size of 512. The model achieves an accuracy of 88.9% on the training set and 87.6% on the test set.

B.2 Additional plots

Figure 8 shows the sizes of the conformal sets obtained for each data batch. Interestingly, the size distribution varies across batches, reflecting not only the influence of the method and the batch position in the sequence but also an intrinsic dependence on the data within each batch. We also empirically observe that the conformal sets tend to grow larger as the position t in the sequence increases. This highlights a limitation of the method: the more we seek simultaneous guarantees, the weaker these guarantees become.

We also visualize examples of batch anytime-valid conformal prediction sets in Figures 9, 11, 13, 15, and 17. The x-axis represents the time steps, while the y-axis corresponds to the different labels. Black cells indicate the conformal sets. For each time step, the true label is marked with a red star. For completeness, we also display the model f 's predictions using green triangles. Additionally, we plot the corresponding martingales M_t in Figures 10, 12, 14, 16, and 18. As expected, the value of the martingale

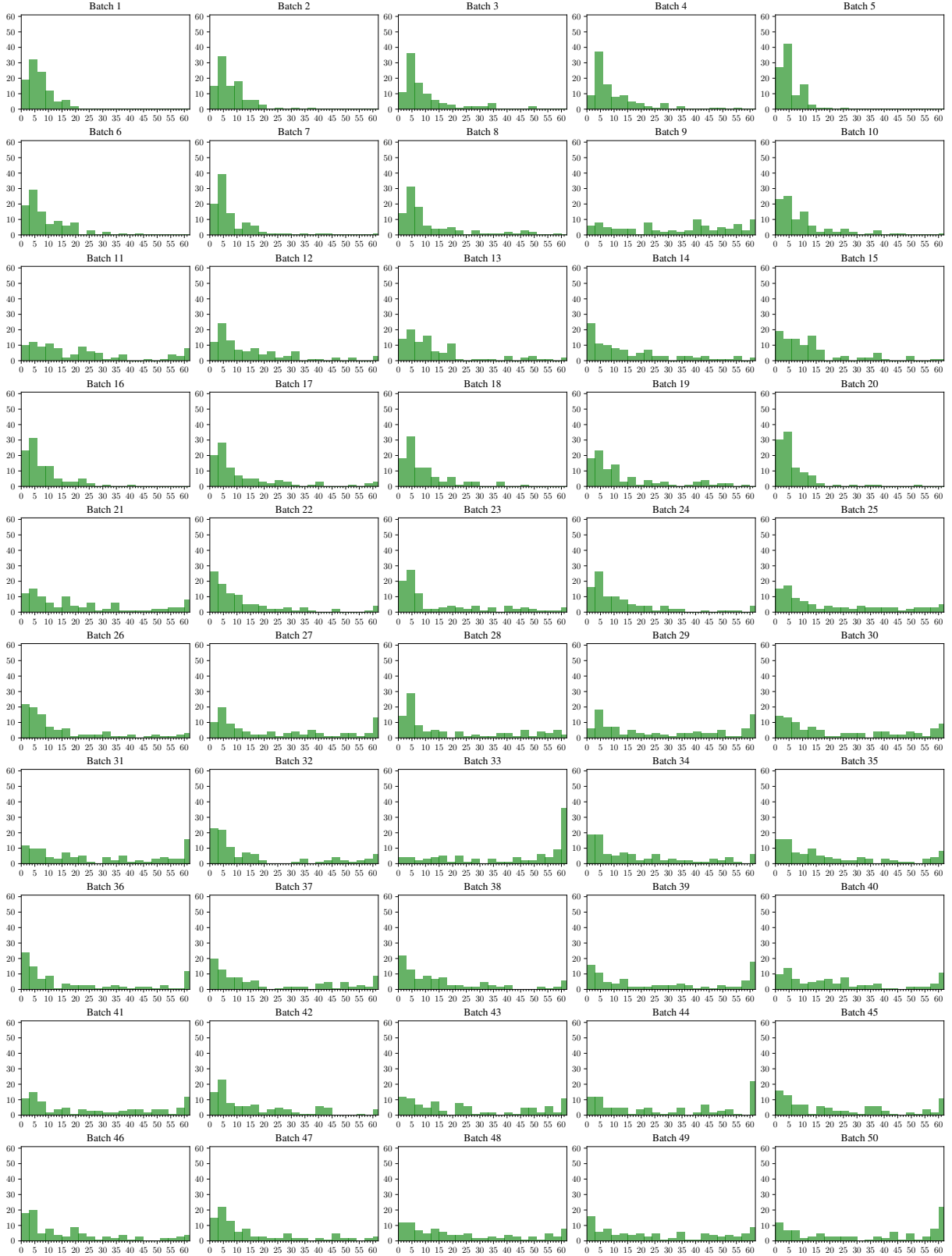


Figure 8: Histograms of conformal set sizes per batch, aggregated over 100 iterations.

M_t significantly influences the quality of the conformal set at time t . When the martingale is close to zero, the conformal sets become larger and less informative.

Interestingly, Figures 17 and 18 illustrate a case where the sequence of batch anytime-valid conformal sets does not fully cover the true labels. This occurs at batches $t = 49$ and $t = 50$.

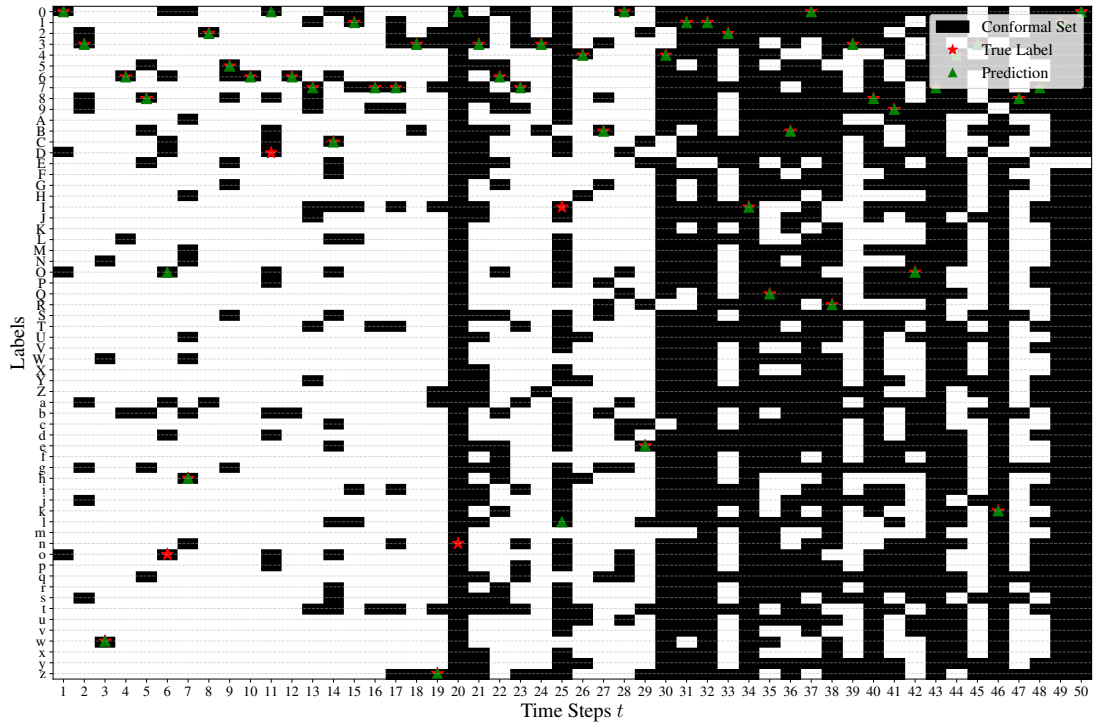


Figure 9: Example 1 of sequence of batch anytime-valid conformal sets.

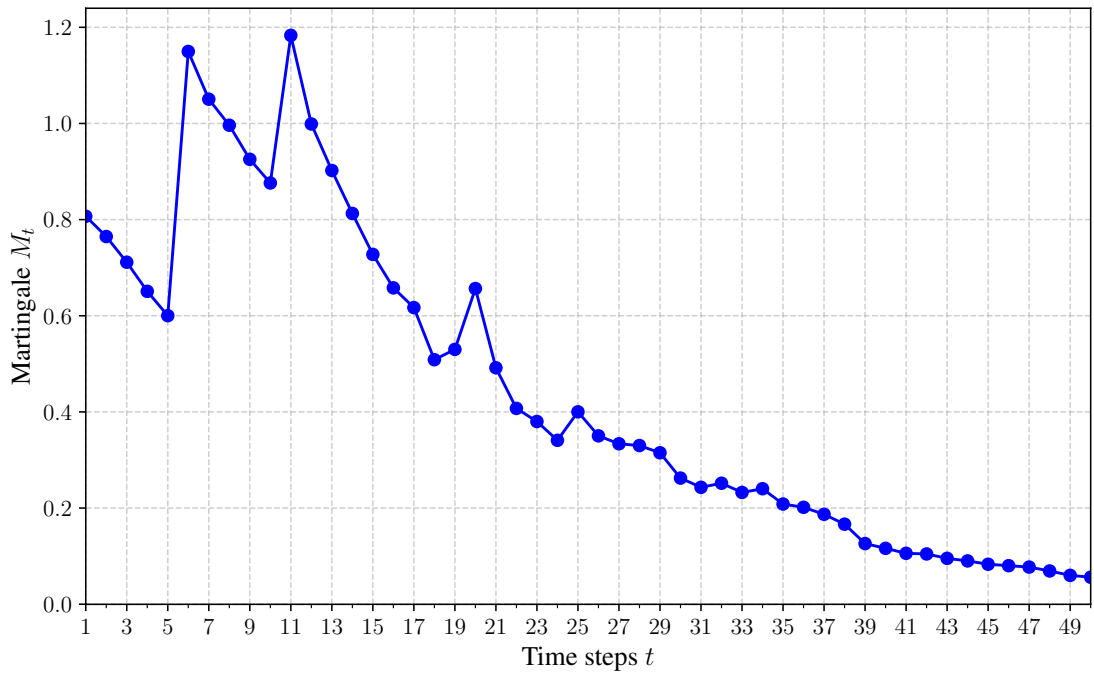


Figure 10: Sample path of the martingale M_t associated with the sequence of batch anytime-valid conformal sets from Example 1.

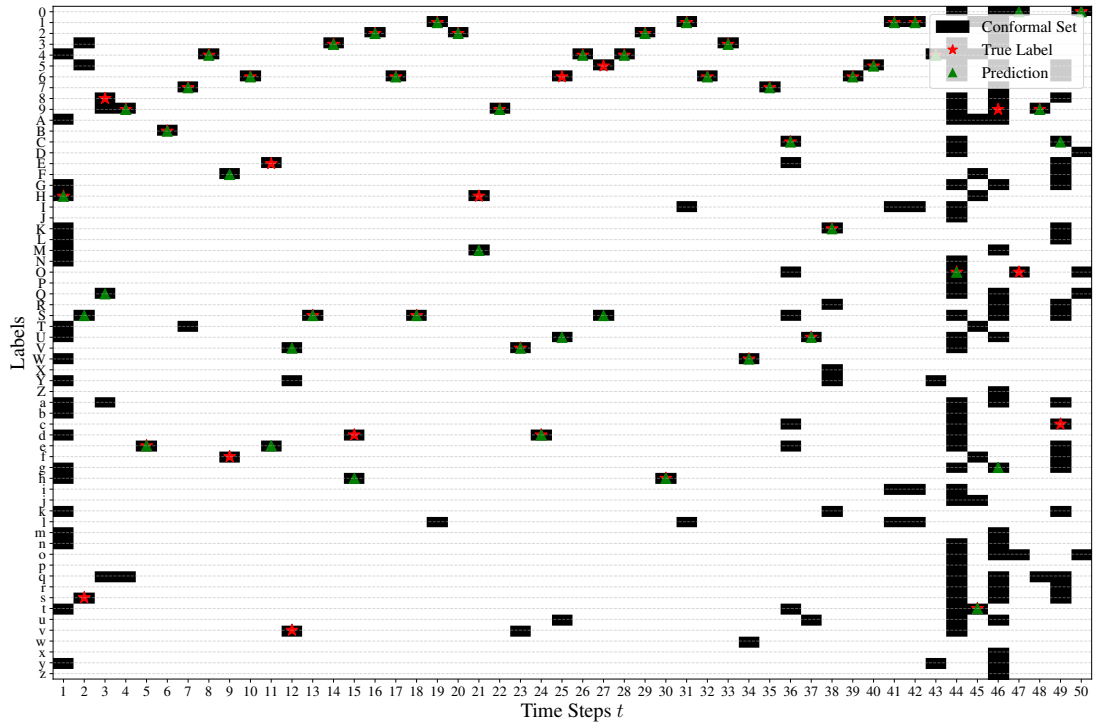


Figure 11: Example 2 of sequence of batch anytime-valid conformal sets.

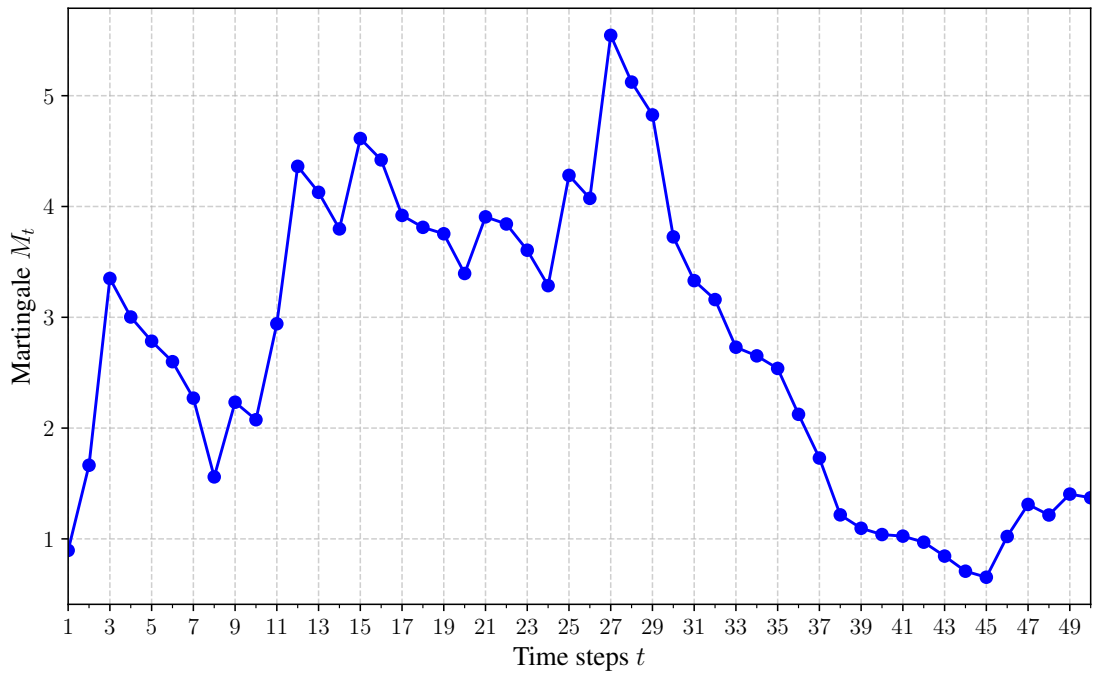


Figure 12: Sample path of the martingale M_t associated with the sequence of batch anytime-valid conformal sets from Example 2.

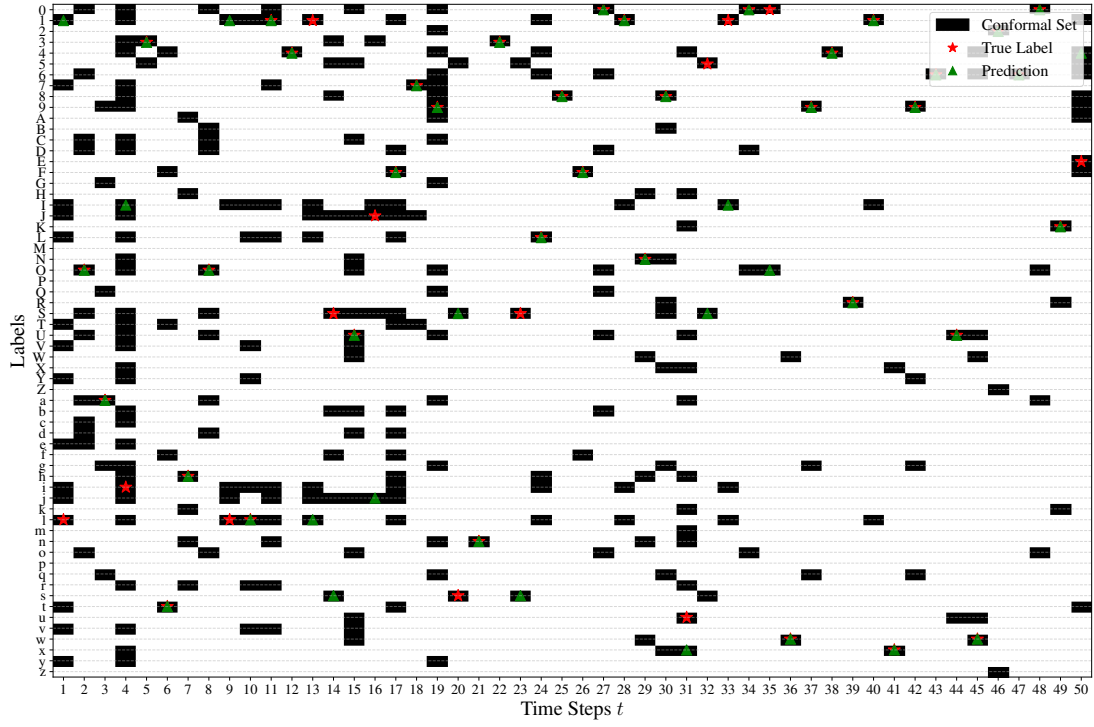


Figure 13: Example 3 of sequence of batch anytime-valid conformal sets.

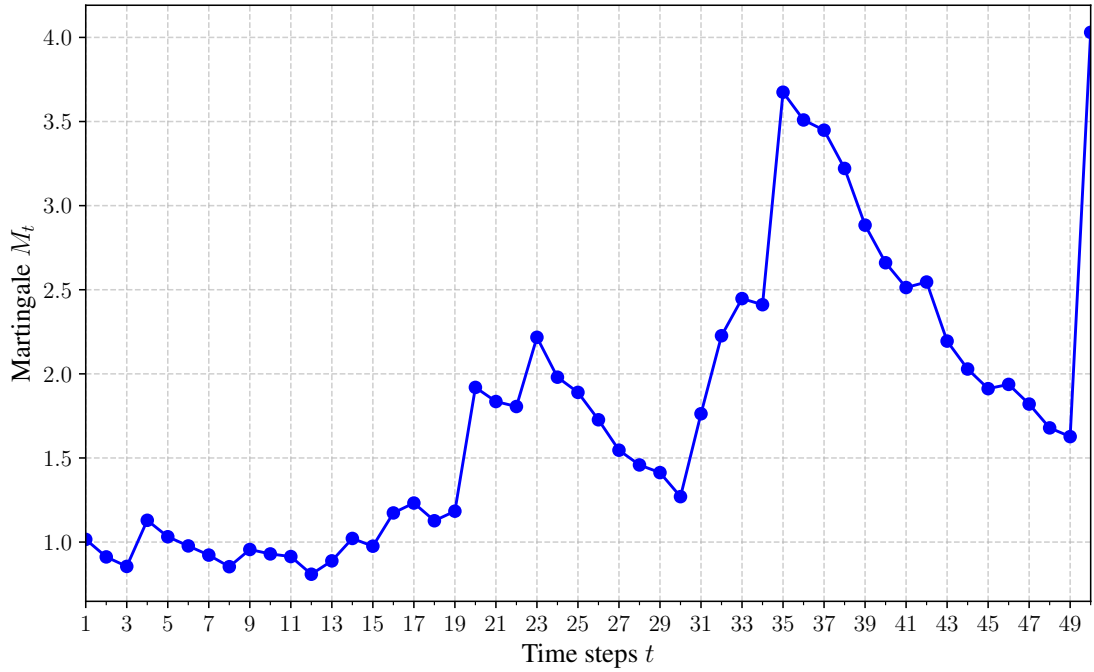


Figure 14: Sample path of the martingale M_t associated with the sequence of batch anytime-valid conformal sets from Example 3.

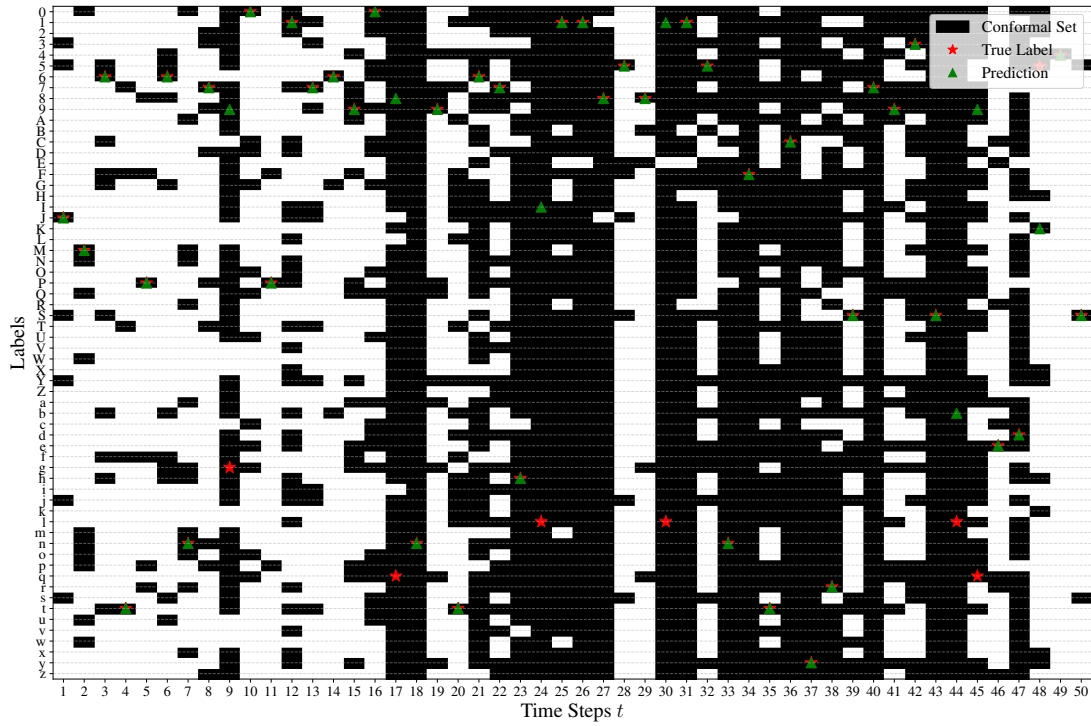


Figure 15: Example 4 of sequence of batch anytime-valid conformal sets.

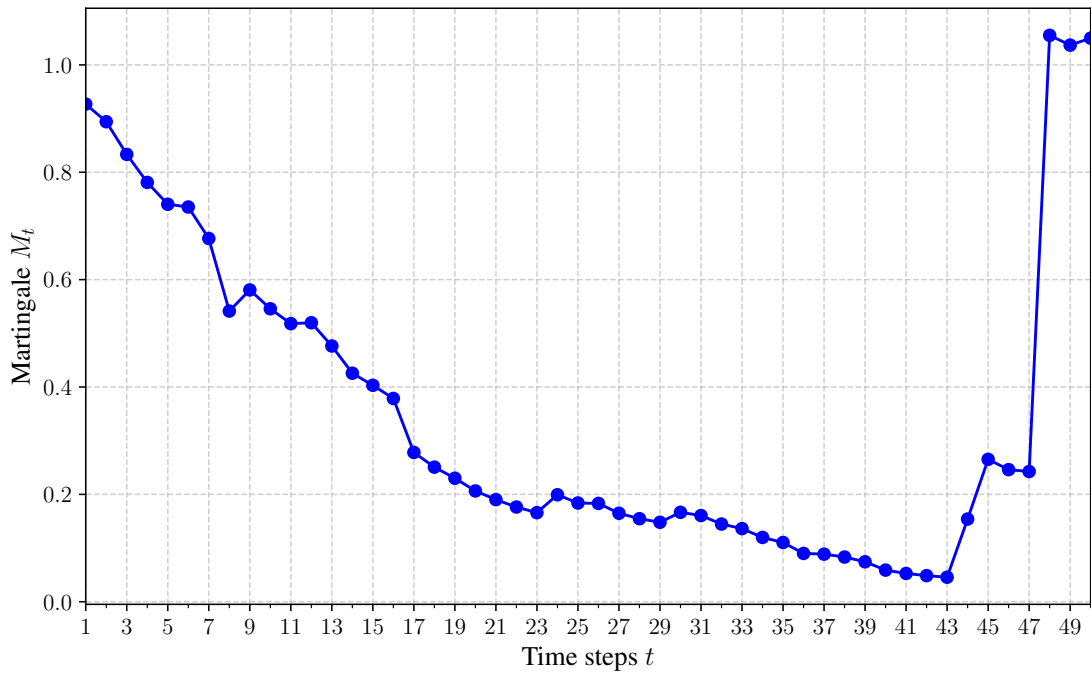


Figure 16: Sample path of the martingale M_t associated with the sequence of batch anytime-valid conformal sets from Example 4.

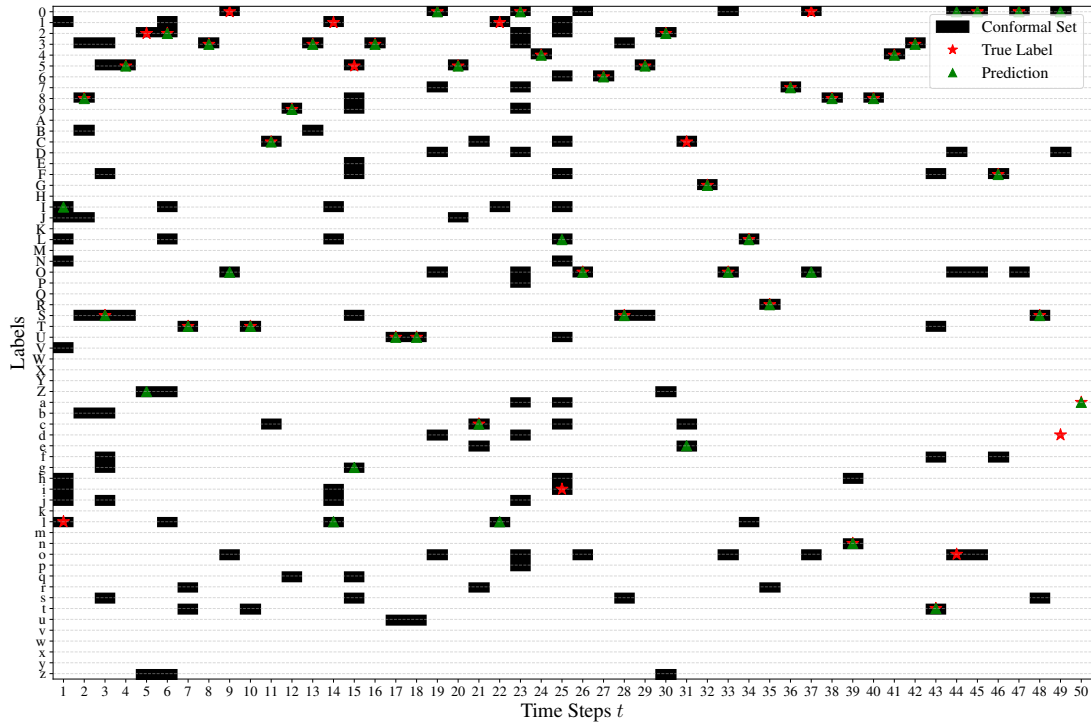


Figure 17: Example 5 of sequence of batch anytime-valid conformal sets.

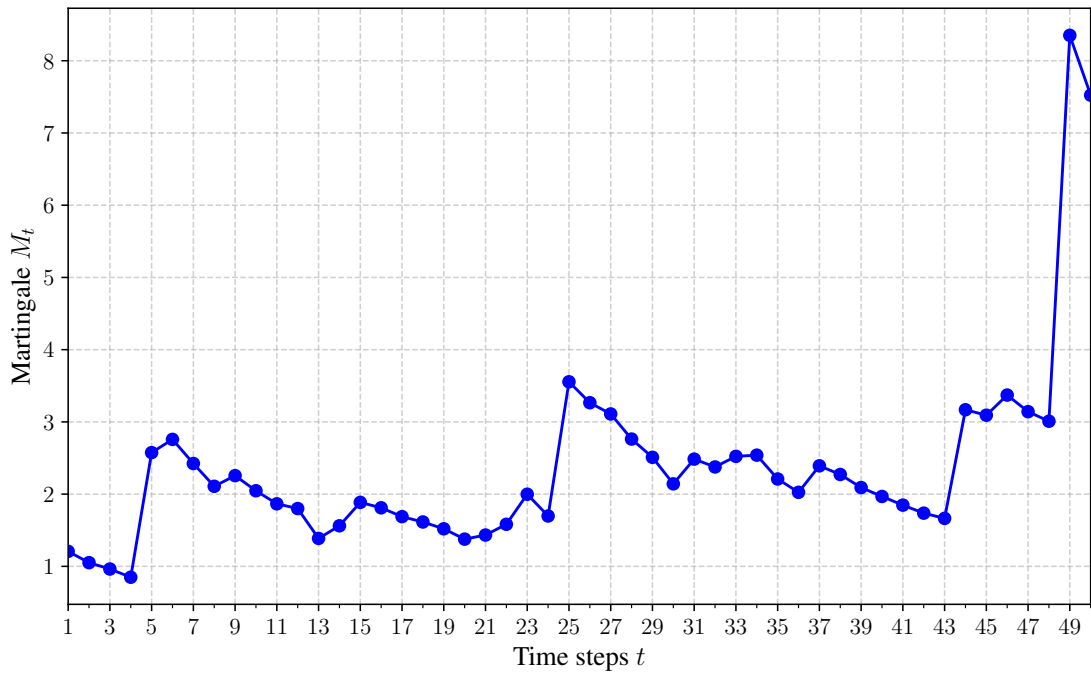


Figure 18: Sample path of the martingale M_t associated with the sequence of batch anytime-valid conformal sets from Example 5.

C Additional Plots for Section 3

We present additional sample results from the experiments in Section 3, in Figure 19 and Figure 20. For example, if we aim to obtain conformal sets with a size (at most) $C = 5$, applying Equation (10) yields $\tilde{\alpha} = 0.11$ in Example 2 of Figure 19, and $\tilde{\alpha} = 0.04$ in Example 3 of Figure 20.

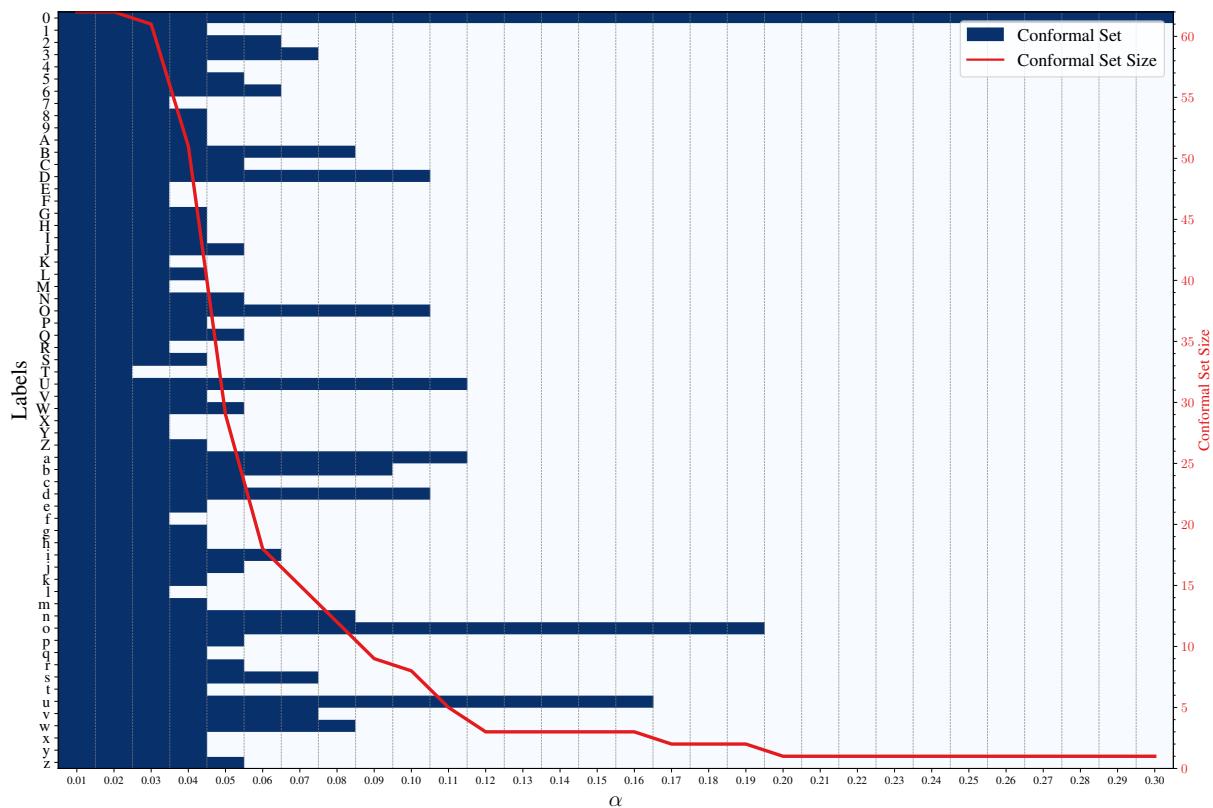


Figure 19: Example 2 of conformal sets obtained with varying $\tilde{\alpha}$.

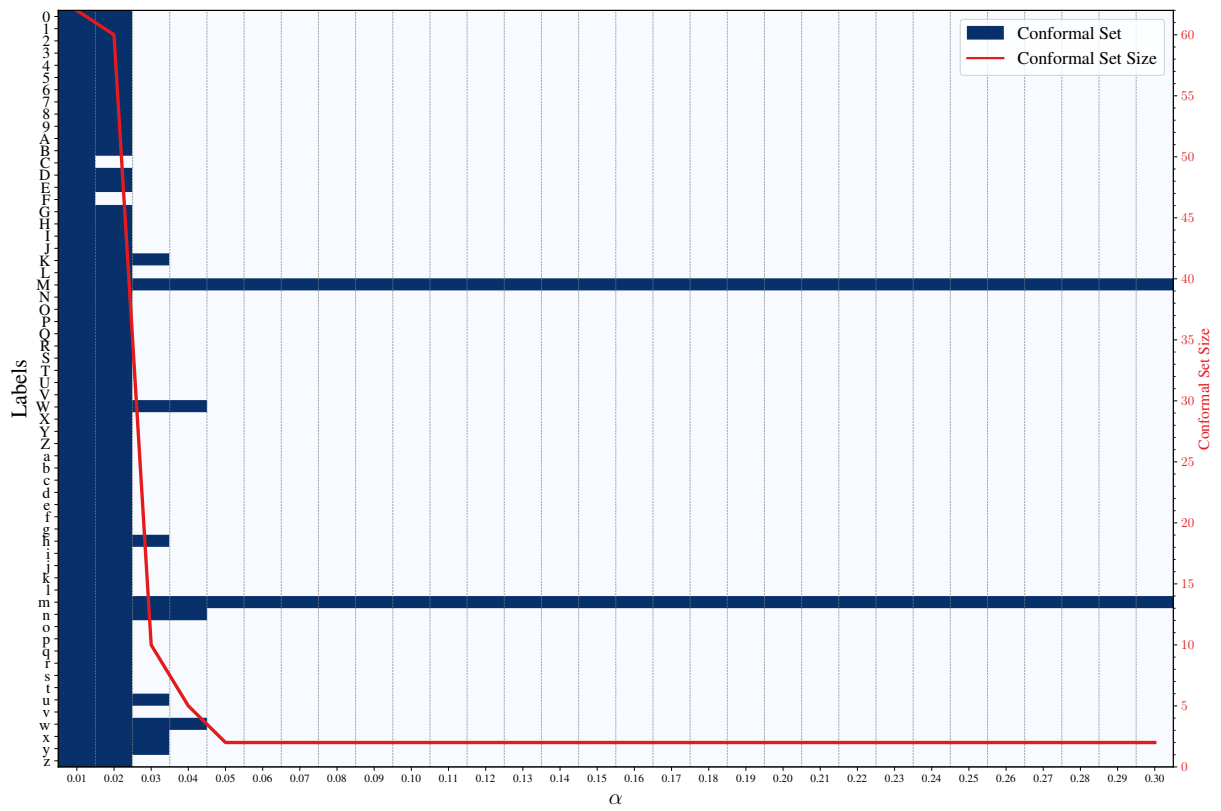


Figure 20: Example 3 of conformal sets obtained with varying $\tilde{\alpha}$.